Study of IEEE 802.16a TDD OFDMA Uplink Channel Estimation

Prepared by Ming-Je Li

Directed by Prof. D. W. Lin

In Partial Fulfillment of the Requirements

for the Degree of
Master of Science

Department of Electronics Engineering

National Chiao Tung University

Hsinchu, Taiwan 300, R.O.C.

E-mail: u870949@micro.ee.nthu.edu.tw

Contents

List of Figures

List of Tables

Chapter 1

Introduction

Communication plays an important rule in human life. Today, communication devices not only provide voice service but also entertainment, such as mutimedia content. Due to the transmission of large digital content, such as video, images, WWW pages, and data, communication technology is being driven to surport high data rate transmission, even real-time transmission in some applications. There has been considerable research effort in recent years aimed at developing high perfermance and high data rate transmission methods.

1.1 Motivation of the Thesis

Because of high-speed data transmission, the system suffers the severe effect of multipath fading which significantly degrades the system performance. In recent years, orthogonal frequency division multiplexing (OFDM) modulation technique has drawn great interest due to its advantage in mitigating the severe effects of frequency-selective fading in high-speed wireless communication. The IEEE 802.16 standard committee has developed a group of standards for wireless MANs. Project 802.16a is one of them. The object of this study is the OFDMA-based interface option of this project, namely WirelessMAN-OFDMA.

In high data rate transmission, the imperfectness of channels, e.g., multipaths,

causes more severe trouble than in low-rate transmission in demodulation. The result of data transmission over such a channel is that each received symbol is affected somewhat by adjacent symbols, thereby bringing about a common form of interference referred to as intersymbol interference (ISI). Intersymbol interference is a major soure which degrades performance in the reconstructed data at receiver. In single carrier transmission, we usually employ an time domain adaptive equalizer to solve this problem. If the channel has very long impulse response compared with symbol duration, time domain equalizer may fail to handle ISI. However, in OFDM system, ISI can be easily eliminated by inserting cyclid prefix which is longer than the maximum delay spread, at the expense of some loss in capacity.

In uncoded OFDM, we only need a frequency domain equalizer with one tap at the receiver for each subcarrier. The purpose of channel estimation is to obtain the channel response at each subcarrier. Then, we can easily abtain the equalizer coefficient, the inverse of the channel gain. In channel coded OFDM, such as that in IEEE 802.16a OFDMA equalization is not needed, but the estimated channel response is directly useful in chnnel decoding [1]. Hence in this thesis, we will investigate channel estimation methods that can be applied to the IEEE 802.16a standard.

1.2 Organization of This Thesis

This thesis is organized as follows. In Chapter 2, we will give an overview for orthogonal frequency division multiplexing(OFDM), which is the technology behind the IEEE 802.16a standard. In addition, we will introduce some conventional channel estimation methods. In Chapter 3, we will propose a channel estimator based on the IEEE 802.16a standard and evaluate the performance of the proposed method. In chapter 4, we try to find a way to track the multipath time delays. Finally, in Chapter 5, we will give a brief conclusion.

Chapter 2

Overview of OFDM and Channel Estimation

In this chapter, we give a brief overview of OFDM. Then we will show why channel estimation is important and introduce some conventional channel estimators. In addition, we will describe the content related to uplink channel specification in IEEE 802.16a, and explain the implicit restrictions.

2.1 Basic Concepts of OFDM

OFDM is a maulticarrier transmission technique based on the discrete Fourier transform (DFT). The basic concept is to divide data into several parallel bit streams and modulate these streams by a set of independent subcarriers [2]. In order to enhance bandwidth efficiency, the spectra of the subcarriers are overlapping and orthogonal. Thus the OFDM system splits the high rate data stream into a mumber of lower rate streams. Hence, we can avoid reducing the symol period to increase the transmitted rate and thus suffering serious frequency selective fading. The parallel data transmission by means of frequency division multiplication (FDM) was proposed in mid-1960s. But until Weinstein proposed to use discrete Fourier transform (DFT) in the baseband modulation and demodulation [3], OFDM modulation entered a new century. This idea largely decreases the complexity of OFDM implementation

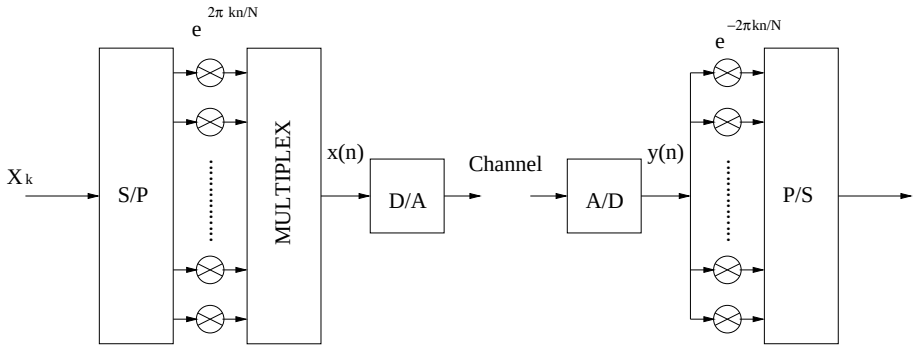

Figure 2.1: Basic concept of OFDM system.

compared with the need of multiple oscillators to modulate.

The basic concepts of OFDMA are the same as those of OFDM. But in addition, OFDMA can surport multiaccess. Active carriers in the OFDMA system are devided into subsets of carriers, each subset is termed a subchannel. A subscriber may be assigned one or more than one subchannels, depending on their requirement. Then, several subscribers share a communication resource, and a system controller can dynamically change the resource allotted to each subscriber.

2.2 Signal Model

The following material is modified from [4]. If we take N_{FFT} subcarriers spread over bandwidth of $N_{FFT} \cdot \Delta f$ Hz, and sub-carrier k is modulated by the transmitted data X_k which is a complex number in a QAM constellation. Then a typical continuous-time OFDM symbol is of the form

$$x(t) = \begin{cases} \sum_{k=-N_{FFT}/2}^{N_{FFT}/2} X_k \cdot e^{j2\pi k \Delta f t}, & 0 < t < T, \\ 0, & \text{otherwise}, \end{cases} \tag{2.1}$$

where T is symbol duration, $e^{j2\pi k \Delta f t}$ is the basis function, and Δf is the carrier frequency spacing which must be large enough to maintain the orthogonality of the

basis functions. We know the least spacing is

$$\Delta f = \frac{1}{T}.$$

Then the inner product of any two basis functions is

$$\int_0^T e^{j2\pi k_2 \Delta f t} \cdot e^{j2\pi k_1 \Delta f t}\, dt = 0, \quad \text{for } k_1 \neq k_2.$$

Furthermore, only N_{FFT} sampling points with sampling rate $\frac{N_{FFT}}{T}$ from $x(t)$ are enough to represent the original data X_k:

$$X_k = \sum_{n=0}^{N_{FFT}-1} x(\frac{nT}{N_{FFT}}) \cdot e^{j2\pi k \Delta f \cdot (\frac{nT}{N_{FFT}})}, \quad k = -N_{FFT}/2, \ldots, N_{FFT}/2.$$

Now, we consider that a sequence of OFDM symbols is transmitted. Then the transmitted signal will be distorted by the communication channel which is dispersive. To avoid time-domain aliasing between adjacent OFDM symbols, we need to separate them from each other with a "guard time" T_g which is at least longer than the entire impulse response of the channel:

$$x(t) = \begin{cases} \sum_{k=-N_{FFT}/2}^{N_{FFT}/2} X_k \cdot e^{j2\pi k \Delta f (t-T_g)}, & T_g < t < T_b + T_g, \\ 0, & \text{otherwise}, \end{cases} \tag{2.2}$$

where T_b is the original useful time and $T_s = T_b + T_g$ is symbol period. Then we lose a litte bandwidth efficiency in order to curtail the interference between adjacent symbols. With the separation of OFDM symbols, we can just consider individual OFDM symbols only. So now we consider one shot transmission of $x(t)$ specified in (2.2). Then we can find that the received signal will be

$$y(t) = x(t) * h(t) \tag{2.3}$$

where $h(t)$ is the channel impulse response. For simplicity, we tentatively ignore the noise effect. And the received signal $y(t)$ will lie inside the range $[T_g,\ T_s + T_g]$.

Transforming (2.3) to the frequency domain, we get

$$Y(e^{j2\pi f}) = X(e^{j2\pi f}) H(e^{j2\pi f}).$$

Recall that the transmitted data are the frequency spectrum of $x(t)$. Now for any frequency the received signal $Y(e^{j2\pi f})$ can be writen as the multiplication of $X(e^{j2\pi f})$ and $H(e^{j2\pi f})$. This result is important for demodulation. We are only concerned about the set of $f = k\Delta f$, $k = -N_{FFT}/2, \ldots, N_{FFT}/2$, where the transmitted data are contained in

$$Y(e^{j2\pi k\Delta f}) = X(e^{j2\pi k\Delta f})H(e^{j2\pi k\Delta f}).$$

The relation between the transmitted data X_k and $X(e^{j2\pi k\Delta f})$ is given by

$$\begin{aligned} X(e^{j2\pi k\Delta f}) &= \int_{T_g}^{T_b+T_g} x(t)\cdot e^{j2\pi k\Delta f}\,dt \\ &= \int_{T_g}^{T_b+T_g} \sum_{l=-N_{FFT}/2}^{N_{FFT}/2} X_l\cdot e^{j2\pi l\Delta f(t-T_g)}\cdot e^{-j2\pi k\Delta f(t-T_g)}\,dt \\ &= T_b\cdot X_k. \end{aligned}$$

Then X_k can be written in terms of $S(e^{j2\pi k\Delta f})$ or $Y(e^{j2\pi k\Delta f})$ as

$$X_k = \frac{1}{T_b}X(e^{j2\pi k\Delta f}) = \frac{1}{T_b}Y(e^{j2\pi k\Delta f})/H(e^{j2\pi k\Delta f}).$$

So in the receiver we need to calculate the Fourier transform of the received signal:

$$\begin{aligned} Y(e^{j2\pi k\Delta f}) &= \int_{T_g}^{T_s+T_g} y(t)\cdot e^{-j2\pi k\Delta f(t-T_g)}\,dt \\ &= \int_{T_g}^{T_s} y(t)\cdot e^{-j\frac{2\pi k(t-T_g)}{T_b}}\,dt + \int_{T_s}^{T_s+T_g} y(t)\cdot e^{-j\frac{2\pi k(t-T_g)}{T_b}}\,dt \\ &= \int_{0}^{T_b} y(t+T_g)\cdot e^{-j\frac{2\pi kt}{T_b}}\,dt + \int_{0}^{T_g} y(t+T_s)\cdot e^{-j\frac{2\pi k(t+T_b)}{T_b}}\,dt. \end{aligned}$$

Since $e^{-j\frac{2\pi kt}{T_b}}$ is T_b-periodic in t, i.e., $e^{-j\frac{2\pi k(t+T_b)}{T_b}} = e^{-j\frac{2\pi kt}{T_b}}$, we get

$$\begin{aligned} Y(e^{j2\pi k\Delta f}) &= \int_{0}^{T_b} y(t+T_g)\cdot e^{-j\frac{2\pi kt}{T_b}}\,dt + \int_{0}^{T_g} y(t+T_s)\cdot e^{-j\frac{2\pi kt}{T_b}}\,dt \\ &= \int_{0}^{T_g} (y(t+T_g)+y(t+T_s))\cdot e^{-j\frac{2\pi kt}{T_b}}\,dt + \int_{T_g}^{T_b} y(t+T_g)\cdot e^{-j\frac{2\pi kt}{T_b}}\,dt \end{aligned}$$

where $y(t+T_s)$ is a "time aliasing term." There is nothing surprising about the "time aliasing term." The process of culculating $Y(e^{j2\pi k\Delta f})$ is similar to Fourier series

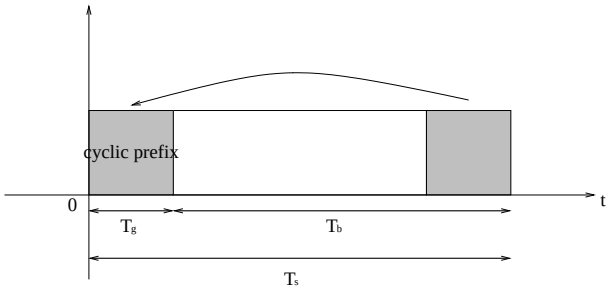

Figure 2.2: OFDM symbol time structure.

representation with period T_b. That is to say, the original signal $y(t)$ is periodically duplicated with period T_b. But the length of the received signal is in the range of $[T_b,\ T_s)$, giving rise to time-aliasing. With further thought, we see that the "time-aliasing term" is needed. If we duplicated with the period T_s, then we get wrong carrier spacing $\Delta f' = \frac{1}{T_s}$.

By linearity, the aliasing term can be achieved at transmitter by adding a copy of the last T_g of useful symbol period, termed cyclic prefix, in front of the original signal. Define a cyclic prefix as below

$$x_{cp}(t) \quad = \quad \begin{cases} x(t+T_b) = \sum\limits_{k=-N_{FFT}/2}^{N_{FFT}/2} X_k \cdot e^{j2\pi k\Delta f(t-T_g)}, & 0 < t < T_g, \\ 0, & \text{otherwise.} \end{cases}$$

Then by means of convolving the cyclic prefix with the channel impulse response, "time-aliasing term" can be obtained. Eventually, the signal model for the OFDM system is given by

$$\widetilde{x}(t) \quad = \quad \begin{cases} \sum\limits_{k=-N_{FFT}/2}^{N_{FFT}/2} X_k \cdot e^{j2\pi k\Delta f(t-T_g)}, & 0 < t < T_s, \\ 0, & \text{otherwise.} \end{cases} \tag{2.4}$$

Note that the range of t has changed compared with (2.2). OFDM symbol time structure is shown in Fig. 2.2. Then the received signal becomes

$$\widetilde{y}(t) = \widetilde{x}(t) * h(t). \tag{2.5}$$

We just retain $\widetilde{y}(t)$ in the range of $[T_g,\ T_s]$ and drop the rest. Then we take the

Fourier transform of the remainder, we can get the whole range of frequency response. Since we only care about N_{FFT} discrete points with equal carrier spacing in frequency domain, we can simplify the process. Just use the N_{FFT} sampling points in time domain. By discrete-time signal processing, we can recover the desired information:

$$Y(e^{j2\pi k\Delta f}) = \sum_{n=0}^{N_{FFT}-1} \widetilde{y}(\frac{nT_b}{N_{FFT}}) \cdot e^{j2\pi k\Delta f \cdot (\frac{nT_b}{N_{FFT}})}, \quad k = -N_{FFT}/2, \ldots, N_{FFT}/2.$$

Now the overall system model is as shown in the Fig. 2.3.

Up to now, we have not yet commpleted the process of restoring the distorted signal. We need the information of the channel response $H(e^{j2\pi k\Delta f})$. That is the main subject of this thesis. The mobile communication channel must be estimated with sufficient accuracy so that the transmitted data can be detected even when a large constellation is used. If not, a high spectal efficiency becomes unattainable. To start, we introduce some conventional channel estimation methods in the next section.

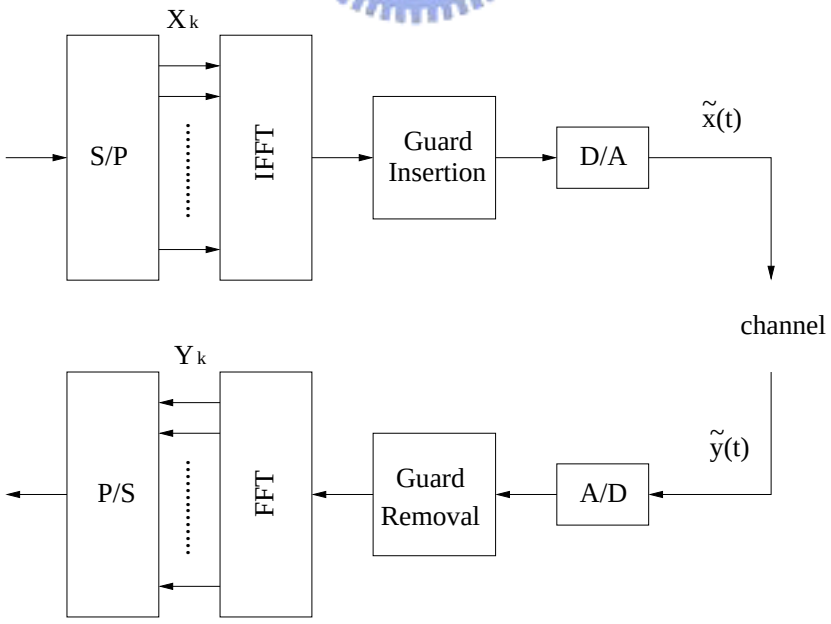

Figure 2.3: OFDM baseband system model.

2.3 Some Conventional Channel Estimation Methods

The material in this section is largely taken from [5].

2.3.1 MMSE Estimation

Let N_{FFT} be the total number of subcarrier in the OFDM system. In matrix notation, we have describe the OFDM system as

$$\begin{bmatrix} Y_0 \\ Y_1 \\ \vdots \\ Y_{N_{FFT}-1} \end{bmatrix} = \begin{bmatrix} X_0 & & & 0 \\ & X_1 & & \\ & & \ddots & \\ 0 & & & X_{N_{FFT}-1} \end{bmatrix} \begin{bmatrix} W_{N_{FFT}}^{0,0} & \cdots & W_{N_{FFT}}^{0,N_{FFT}-1} \\ W_{N_{FFT}}^{1,0} & & \\ \vdots & \ddots & \\ W_{N_{FFT}}^{N_{FFT}-1,0} & \cdots & W_{N_{FFT}}^{N_{FFT}-1,N_{FFT}-1} \end{bmatrix} \times \begin{bmatrix} h_0 \\ h_1 \\ \vdots \\ h_{N_{FFT}-1} \end{bmatrix} + \begin{bmatrix} \widetilde{N}_0 \\ \widetilde{N}_1 \\ \vdots \\ \widetilde{N}_{N_{FFT}-1} \end{bmatrix}, \tag{2.6}$$

or

$$\mathbf{Y} = \mathbf{XFh} + \widetilde{\mathbf{N}}, \tag{2.7}$$

where $\mathbf{Y}$ is the received vector, $\mathbf{X}$ is a diagonal matrix containing the transmitted data or pilots and $\mathbf{F}$ is discrete Fourier transform matrix with

$$W_N^{i,j} = e^{-j\frac{2\pi ij}{N}}, \tag{2.8}$$

$\mathbf{h}$ is the channel impulse response vector, and $\widetilde{\mathbf{N}}$ is a vector of complex AWGN.

Suppose that the transmitted data X_k, where $k = \{0, 1, \cdots, N_{FFT} - 1\}$, are either training symbol or detected variable in a decision feedback estimator. Then, by minimum mean square error criterion, the estimated values of the channel impuse response will be [5]

$$\widehat{\mathbf{h}} = \mathbf{R_{hY}} \mathbf{R_{YY}^{-1}} \mathbf{Y} \tag{2.9}$$

where

$$\begin{aligned}\mathbf{R_{hY}} &= E[\mathbf{hY}^H] = \mathbf{R_{hh}F}^H\mathbf{X}^H, \\ \mathbf{R_{YY}} &= E[\mathbf{YY}^H] = \mathbf{XFR_{hh}F}^H\mathbf{X}^H + \mathbf{R_{\widetilde{N}\widetilde{N}}},\end{aligned}$$

with $\mathbf{R_{hh}}$ being the auto-covariance matrix of $\mathbf{h}$ and $\mathbf{R_{\widetilde{N}\widetilde{N}}}$ the auto-covariance matrix of $\widetilde{\mathbf{N}}$.

Note that there is a matrix inversion, with size N_{FFT}, which incurs a high complexity. In order to make MMSE estimator efficient, we observe the channel property. The main energy concentrates in the first M taps which is approximately the size of cyclic prefix. If we just consider the first M taps of h, then a modified MMSE estimator can save a lot of multiplications. The overall derivation and the final result can be found in [5], which we omit.

In addition, the second order statistics must be either assumed fixed or estimated by collecting recent data. In other words, MMSE estimator is applicable to communication through slowly time variant channels. Then the statistics can be viewed as quasi-stationary.

In fact, the communication channel may be fast-fading depending on the velocity of mobile. So we must adapt the auto-correlation of channel and estimate the channel in real time. For the sake of real-time requirement, we cannot depend only on the training symbols. Hence, each OFDM symbol is inserted pilot carriers, which the receiver knows, to assist channel estimation. The pilots are multiplexed into the transmitted data stream, so the channel gains at pilot locations can be estimated. The channel responses at data locations can be obtained by interpolation.

First, we assume there are M subcarriers chosen from the original N_{FFT} subcarriers to be used as pilots. Define $\{i_0, i_1, \cdots, i_{M-1}\}$ as the indexes of pilots. Then (2.6) can be rewritten with only pilots as

$$\begin{bmatrix} Y_{i_0} \\ Y_{i_1} \\ \vdots \\ Y_{i_{M-1}} \end{bmatrix} = \begin{bmatrix} X_{i_0} & & & 0 \\ & X_{i_1} & & \\ & & \ddots & \\ 0 & & & X_{i_{M-1}} \end{bmatrix} \begin{bmatrix} W_{N_{FFT}}^{i_0,0} & \cdots & W_{N_{FFT}}^{i_0,N_{FFT}-1} \\ W_{N_{FFT}}^{i_1,0} & & \\ \vdots & \ddots & \\ W_{N_{FFT}}^{i_{M-1},0} & \cdots & W_{N_{FFT}}^{i_{M-1},N_{FFT}-1} \end{bmatrix} \begin{bmatrix} h_0 \\ h_1 \\ \vdots \\ h_{N_{FFT}-1} \end{bmatrix} + \begin{bmatrix} \widetilde{N}_{i_0} \\ \widetilde{N}_{i_1} \\ \vdots \\ \widetilde{N}_{i_{M-1}} \end{bmatrix}. \tag{2.10}$$

For decreasing the complexity, we just take into account the first M taps of h, and set the others zeros, just as mentioned in [5]. Then we can get

$$\mathbf{Y}_p = \mathbf{X}_p \mathbf{F}_p \mathbf{h}' + \widetilde{\mathbf{N}}_p \tag{2.11}$$

where $\mathbf{h}' = [h_0 \; h_1 \; \cdots \; h_{M-1}]^T$ and

$$\mathbf{F}_p = \begin{bmatrix} W_{N_{FFT}}^{i_0,0} & \cdots & W_{N_{FFT}}^{i_0,M-1} \\ W_{N_{FFT}}^{i_1,0} & & \\ \vdots & \ddots & \\ W_{N_{FFT}}^{i_{M-1},0} & \cdots & W_{N_{FFT}}^{i_{M-1},M-1} \end{bmatrix}.$$

Through a similar derivation as that led to 2.9, we get the optimal solution as

$$\widehat{\mathbf{h}}' = \mathbf{R}_{\mathbf{h}'\mathbf{Y}_p} \mathbf{R}_{\mathbf{Y}_p\mathbf{Y}_p}^{-1} \mathbf{Y}_p \tag{2.12}$$

where

$$\begin{aligned} \mathbf{R}_{\mathbf{h}'\mathbf{Y}_p} &= E[\mathbf{h}'\mathbf{Y}_p^H] = \mathbf{R}_{\mathbf{h}'\mathbf{h}'} \mathbf{F}_p^H \mathbf{X}_p^H, \\ \mathbf{R}_{\mathbf{Y}_p\mathbf{Y}_p} &= E[\mathbf{Y}_p\mathbf{Y}_p^H] = \mathbf{X}_p \mathbf{F}_p \mathbf{R}_{\mathbf{h}'\mathbf{h}'} \mathbf{F}_p^H \mathbf{X}_p^H + \mathbf{R}_{\widetilde{\mathbf{N}}_p\widetilde{\mathbf{N}}_p}, \end{aligned}$$

with $\mathbf{R}_{\mathbf{h}'\mathbf{h}'}$ being the auto-covariance matrix of $\mathbf{h}'$ and $\mathbf{R}_{\widetilde{\mathbf{N}}_p\widetilde{\mathbf{N}}_p}$ the auto-covariance matrix of $\widetilde{\mathbf{N}}_p$. Then we can get the channel gains at other locations by transforming the time domain impulse response to frequency domain. That is, let

$$\widehat{\mathbf{h}} = [\widehat{\mathbf{h}}'^T \overbrace{00 \ldots 0}^{N-M}]^T.$$

Then

$$\widehat{\mathbf{H}} = \mathbf{F}\widehat{\mathbf{h}} \tag{2.13}$$

where $\widehat{\mathbf{H}}$ is the estimated channel response in frequency domain.

2.3.2 LMMSE Estimation

We also introduce an another form of MMSE method to estimate the channel. In (2.12), $\widehat{\mathbf{h}}'$ is the estimated channel impulse response. we can directly estimate the channel frequency response. For convenience, define

$$\widehat{\mathbf{H}}_{p,ls} = [\frac{Y_{i_0}}{X_{i_0}} \ \frac{Y_{i_1}}{X_{i_1}} \ \cdots \ \frac{Y_{i_{M-1}}}{X_{i_{M-1}}}]. \tag{2.14}$$

The channel frequency response at pilot location can be roughly estimated in this way. There exists a linear interpolation method to estimate the overall channel frequency response through $\widehat{\mathbf{H}}_{p,ls}$. Then by minimum mean square error criterion, we can get [6]

$$\widehat{\mathbf{H}} = \mathbf{R}_{\mathbf{H}\widehat{\mathbf{H}}_{p,ls}} \mathbf{R}^{-1}_{\widehat{\mathbf{H}}_{p,ls}\widehat{\mathbf{H}}_{p,ls}} \widehat{\mathbf{H}}_{p,ls} \tag{2.15}$$

where

$$\begin{aligned} \mathbf{R}_{\mathbf{H}\widehat{\mathbf{H}}_{p,ls}} &= \mathbf{R}_{\mathbf{H}\mathbf{H}_{p,ls}}, \\ \mathbf{R}_{\widehat{\mathbf{H}}_{p,ls}\widehat{\mathbf{H}}_{p,ls}} &= \mathbf{R}_{\mathbf{H}_{p,ls}\mathbf{H}_{p,ls}} + \mathbf{R}_{\tilde{\mathbf{N}}_p\tilde{\mathbf{N}}_p}(\mathbf{X}_p\mathbf{X}_p^H)^{-1}. \end{aligned}$$

If the value of the pilot modulation does not change, then the inversion of $\mathbf{X}_p\mathbf{X}_p^H$ is executed once. If $\mathbf{X}_p$ changes for some reasons, then we can average over it. Hence, we replace the term with its expectation $E[\mathbf{X}_p\mathbf{X}_p^H]$. Furthermore, the term $\mathbf{R}_{\widehat{\mathbf{H}}_{p,ls}\widehat{\mathbf{H}}_{p,ls}}$ can be rewritten as

$$\mathbf{R}_{\widehat{\mathbf{H}}_{p,ls}\widehat{\mathbf{H}}_{p,ls}} = \mathbf{R}_{\mathbf{H}_{p,ls}\mathbf{H}_{p,ls}} + \frac{\beta}{SNR}\mathbf{I}$$

where $\beta = E\{|X_{i_k}|^2\}E\{|1/X_{i_k}|^2\}$ for all k. Then the inversion of the matrix $\mathbf{R}_{\widehat{\mathbf{H}}_{p,ls}\widehat{\mathbf{H}}_{p,ls}}$ needs to be calculated only once.

2.3.3 Decision-Directed Channel Estimation

In general, decision-directed approach is to use detected data to fine-tune the estimated channel response for the detection of the next symbol, such as

$$\begin{aligned} \widehat{X}_k(n) &= \frac{Y_k(n)}{\widehat{H}_k(n-1)}, \\ \widehat{H}_k(n) &= \frac{Y_k(n)}{\overline{X}_k(n)}, \end{aligned} \tag{2.16}$$

where n is the symbol index and k is the carrier index. Moreover, $\widehat{X}_k(n)$ is the noisy data before decision and $\overline{X}_k(n)$ is the data after decision. Finally, $\widehat{H}_k(n)$ is the estimated channel response for subcarrier k at time n.

Note that the decision-directed approach contains two features. First, the performance of decision-directed approach depends on the correctness of the detected data. So the decision-directed algorithm operates well at high SNR. For low SNR, there may be error propagation effect. This means we use wrong decision data to modify the channel response, and lead to more errors. It needs some preprocessing to decrease the probability of wrong decisions. In other words, the basic estimator needs to be modified for good performance. For example, we may try to find the best way to decrease noise before using decision-directed estimator. We believe that the overall performance will be dominated by the preprocessing.

Second, because the output of the decision of channel estimator is used by the next symbol, the channel must not change violently. That is, if channel is slowly time-variant, the performance will not be bad. We may take time average to reduce the influence of AWGN for slow-fading channel, e.g.,

$$\alpha\widehat{H}_k(n-1) + \beta\widehat{H}_k(n) = \widehat{H_{ak}}(n).$$

We may conclude that pure decision-directed estimation is not suitable for fast fading channels. For this kind of channels, the estimator must compensate the time variant effect in advance.

2.4 Overview of Uplink Channel in the IEEE 802.16a OFDMA

For the purpose of providing a wide deployment, considerable capacity, high speed, and low cost solution for broadband wireless access, The IEEE 802.16 Working Group created the IEEE standard 802.16 to support point-to-multipoint transmission at data rates up to 120 Mbps. But the transmission environment must be line of sight and has negligible multipath propagation. To accommodate non-line of sight access over low frequencies, IEEE standard 802.16a improves IEEE standard 802.16-2001 by providing more physical layer specifications in support of broadband wireless access at frequencies from 2–11 GHz. The medium access control layer is amended to support multiple physical layer specifications optimized for the frequency bands of application. The standard includes particular physical layer specifications applicable to systems operating between 2 and 11 GHz.[7].

2.4.1 Frequency Domain and Time Domain Descriptions

An OFDMA symbol is composed of carriers. There are several carrier types:

- data carriers for data transmission,
- pilot carriers for various estimation purposes, and
- null carriers that does no transmission at all. They include guard bands and the DC carrier.

Guard band, a narrow frequency band between adjacent channels in multiplexing, is kept unused to prevent the channels from overlapping and causing crosstalk among modulated signals.

In the OFDMA mode, active carriers are partitioned into groups of contiguous carriers. Each subchannel picks one carrier from each of these groups. The symbol

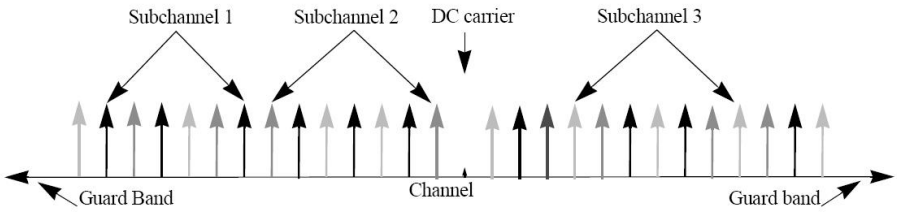

Figure 2.4: OFDMA frequency description (3 channel schematic example) from [7].

is divided into logical subchannels to support multiaccess, and the carriers forming one subchannel may not be adjacent. The conceipt is illustrated in Fig. 2.4

An OFDMA symbol through inverse-Fourier-transform creats the OFDMA waveform. The time duration is known as the useful symbol time T_b. A copy of the last T_g of the useful symbol is used as cyclic prefix. We insert the cyclic prefix in front of an OFDMA symbol. This provides multipath immunity at the cost of some power loss and bandwidth efficiency.

2.4.2 OFDMA Symbol Parameters and Transmitted Signal

The following paragragh is taked from the IEEE 802.16a standard [7].

* Primivie parameters
  - BW: This is the actual transmission bandwidth.
  - F_s/BW: This is the ratio of "sampling frequency" to the nominal transmission bandwidth, set to be 8/7.
  - T_g/T_b: This is the ratio of CP (cyclic prefix) time to "useful" time, where the following values shall be supported: 1/32, 1/16, 1/8, and 1/4.
  - N_{FFT}: This is the number of points for FFT implementation, set as 2048.
* Derived patameters

Table 2.1: OFDM/OFDMA Channelization Parameters for License-Exempt Bands [7]

			OFDM	OFDMA
	F_s/BW		8/7	8/7
BW(MHz)	N_{FFT}		256	2048
10	Δf(kHz)		$44\frac{9}{14}$	$5\frac{47}{81}$
	$T_b(\mu s)$		$22\frac{2}{5}$	$179\frac{1}{5}$
	$T_g(\mu s)$	$\frac{T_b}{32}$	$\frac{7}{10}$	$5\frac{3}{5}$
		$\frac{T_b}{16}$	$1\frac{2}{5}$	$11\frac{1}{5}$
		$\frac{T_b}{8}$	$2\frac{4}{5}$	$22\frac{2}{5}$
		$\frac{T_b}{4}$	$5\frac{3}{5}$	
20	Δf(kHz)		$89\frac{2}{7}$	$11\frac{9}{56}$
	$T_b(\mu s)$		$11\frac{1}{5}$	$89\frac{2}{5}$
	$T_g(\mu s)$	$\frac{T_b}{32}$		$2\frac{4}{5}$
		$\frac{T_b}{16}$	$\frac{7}{10}$	$5\frac{3}{5}$
		$\frac{T_b}{8}$	$1\frac{2}{5}$	$11\frac{1}{5}$
		$\frac{T_b}{4}$	$2\frac{4}{5}$	$22\frac{2}{5}$

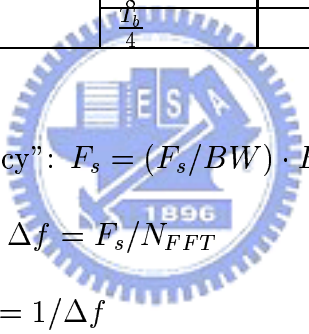

– "Sampling Frequency": $F_s = (F_s/BW) \cdot BW$.

– "Carrier Spacing": $\Delta f = F_s/N_{FFT}$

– "Useful Time": $T_b = 1/\Delta f$

– "Cyclic Prefix Time": $T_g = (T_g/T_b) \cdot T_b$

– "OFDM Symbol Time": $T_s = T_b + T_g$

In our OFDMA study, we choose the transmission bandwidth to be 10 MHz. Then, the "sampling frequency" is $11\frac{3}{7}$ MHz and T_b (useful time), which is the inverse of "carrier spacing," is $179\frac{1}{5}$ μs. Further, we let $\frac{T_g}{T_b} = \frac{1}{8}$, so T_g (cyclic prefix) is $22\frac{2}{5}$ μs and T_s (OFDM symbol time) is $201\frac{3}{5}$ μs. These implementation parameters are chosen from Table 2.1.

The transmitted signal voltage to the antenna is of the form

Table 2.2: OFDMA Uplink Carrier Allocation (from [7])

Parameters	Value
Number of DC carriers	1
Number of Guard Carriers, Left	176
Number of Guard Carriers, Right	175
N_{used}, Number of Used Carriers	1696
Total Number of Carriers	2048
$N_{subchannels}$	32
$N_{subcarriers}$	53
Number of data carriers per subchannel	48
$\{PermutationBase_0\}$	$\{3, 18, 2, 8, 16, 10, 11, 15, 26, 22, 6, 9, 27, 20, 25, 1, 29, 7, 21, 5, 28, 31, 23, 17, 4, 24, 0, 13, 12, 19, 14, 30\}$

$$x(t) = \Re\left\{ e^{j2\pi f_c t} \sum_{\substack{k=-N_{used}/2 \\ k\neq 0}}^{N_{used}/2} X_k \cdot e^{j2\pi k\Delta f(t-T_g)} \right\}, \quad \text{with } 0 < t < T_s, \tag{2.17}$$

where X_k is the complex number data transmitted on the carrier whose frequency offset index is k (it specifies a point in a QAM constellation) and N_{used} is the number of active carriers, including data carriers and pilot carriers.

2.4.3 OFDMA Carrier Allocation

We obtain the set of "used" carriers N_{used} by subtracting the DC carrier and the guard tones from N_{FFT}. These "used" carriers are allocated to two sets of pilot carriers and data carriers for both uplink and downlink. Because this thesis focuses on the uplink channel estimation, we just give the information of the uplink carrier allocation. The "used carriers" are first partitioned into $N_{subchannels}$ subchannels, and then pilots are assigned for each subchannel. To allocate the subchannel, the "used carriers" are divided into $N_{subcarrier}$ groups of contiguous carriers. Each subchannel picks one carrier from each of these groups. Hence each subchannel

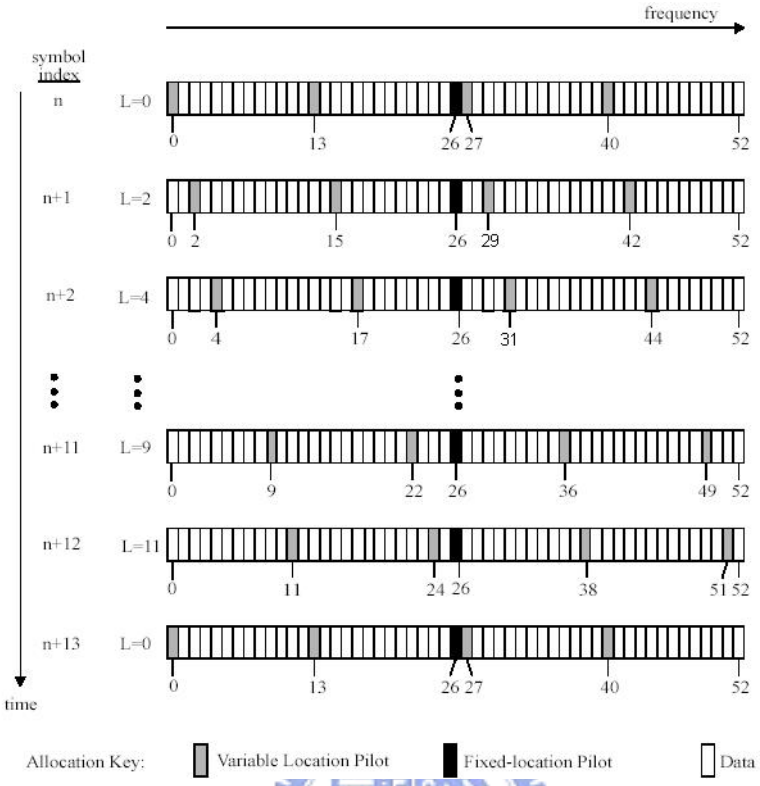

Figure 2.5: Carrier allocations within each OFDMA uplink subchannel [7].

contains $N_{subcarrier}$ subcarriers. So the total number of "used carriers" is equal to $N_{subchannels} \cdot N_{subcarrier}$. Picking which one is according to a permutation formula:

$$\begin{aligned} carrier(n,s) &= N_{subchannels} \cdot n + \{p_s\left[n \bmod (N_{subchannels})\right] \\ &\quad + ID_{cell} \cdot ceil\left[(n+1)/N_{subchannels}\right]\} \bmod (N_{subchannels}) \end{aligned} \quad (2.18)$$

where

$carrier(n,s)$ = carrier index of carrier n in subchannel s.

s = index number of a subchannel, from the set $\{0,\ldots,N_{subchannel}-1\}$.

n = carrier-in-subchannel index form the set $\{0,\ldots,N_{subcarriers}-1\}$.

$p_s[j]$ = the series obtained by rotating $\{PermutationBase_0\}$ cyclically to the left s times.

$ceil[\cdot]$ = function which rounds its argument up to the next integer.

ID_{cell} = a positive integer assigned by the MAC to identify base-station cell.

$X_{\bmod k}$ =the remainder to the quotient X/k.

Clearly, through the permutaion formula, subcarriers for a subchannel are not equally spaced. For each subchannel, there are 48 data carriers, 1 fixed-location pilot carrier, and 4 variable-location pilot carriers. In order to avoid allocating a long term fading location to pilot carriers, the variable-location pilots change with each symbol. And they repeat every 13 OFDM symbols, indexed by $L = 0, \cdots, 12$ which shown in Fig. 2.5. For $L = 0$ the variable location pilots are positioned at indices 0, 13, 27, and 40. For other L these locations change by adding L to index. Note that L is not simply incremented with each symbol, but follows the sequence: 0, 2 , 4, 6, 8, 10, 12, 1, 3, 5, 7, 9, 11.

2.4.4 Pilot Modulation

Pilot carriers shall be inserted into each data burst so as to assist channel estimation. Hence, they are modulated depending on their locations within the OFDMA symbol. In order to keep PAPR (peak-to-average power ratio) low, the pilot data use a sequence, ω_k, generated by the PRBS generator. The polynomial for the PRBS generator is $X^{11} + X^9 + 1$. The value of ω_k is the value of the pilot modulation on the carrier k. For uplink transmission, the initialization vector of the PRBS is: [10101010101]. The PRBS is initialized so that its first output bit coincides with the first usable carrier (as defined in Table 2.2). For the PRBS allocation, the DC carrier and the guard band carriers are not considered as usable carriers. Each pilot is boosted 2.5 dB over the average power of each data tone in ordinary OFDM symbol. The pilot carriers are modulated according to

$$\Re\{c_k\} = \frac{8}{3}(\frac{1}{2} - w_k), \quad \Im\{c_k\} = 0. \tag{2.19}$$

The pilots are not be boosted in the preamble in order to prevent high peak power. That is because the subcarriers in the preamble are all pilots, and there are no data

carriers. Pilots in the preamble are modulated according to

$$\Re\{c_k\} = 2(\frac{1}{2} - w_k), \quad \Im\{c_k\} = 0. \tag{2.20}$$

2.5 Challenge of Uplink Channel Estimation

Our goal is to design a channel estimator corresponding to the specifications in the standard. We have introduced some conventional channel estimation methods. LMMSE is a well known channel estimator. But it needs the statistics of the channel. Therefore, the LMMSE estimator works under the quasi-stationay channels. Intuitively, we expect that the performance is affected by the number of pilot carriers. From a viewpoint in information theory, the more pilot carriers the system has, the more information is revealed to the estimator.

Another approach we consider is the linear interpolation, which is more sensitive to the number of pilot carriers. Fewer pilot carriers results in larger pilot spacings in frequency domain, which may exceed the coherent bandwidth of the channel. Hence, the estimated channel may be far from the actual one. Linear interpolation is a simple way of curve fitting.

Now we consider how many pilot carriers can be supplied for up-link transmission in the standard. We assume that each subscriber are allotted one subchannel. However each subchannel has only 53 subcarriers. But unfortunately, there are 48 data carriers which contain unknown data. Only when the data have been detected can we use the 48 received data to assist in estimating the channel unless some kind of blind algorithm is used. By having only 5 pilot carriers, we must often be confronted with the problem of too few pilot carriers to estimate the channel. The performance may be very poor.

If we only use 5 pilot carriers for interpolation, then on average we can only estimate the channel whose coherent bandwidth is larger than $\frac{BW}{5}$. In other words,

Table 2.3: COST207 6-Ray Models for Macrocellular GSM (Simplified)

Typical Urban		Bad Urban	
Delay(μs)	Fractional Power	Delay(μs)	Fractional Power
0.0	0.189	0.0	0.164
0.2	0.379	0.3	0.293
0.5	0.239	1.0	0.147
1.6	0.095	1.6	0.094
2.3	0.061	5.0	0.185
5.0	0.037	6.6	0.117

the longest delay path of the channel cannot exceed about 0.5 μs according to our implementation parameters. In fact, the delay spread of the communication channel in real world is in the range of 5–7 μs , which is shown in Table 2.3. Hence, we must modify the conventional estimator or propose a new method.

Chapter 3

Channel Estimation for IEEE 802.16a OFDMA Uplink Transmission

In the previous chapter, we have given a brief introdution to the IEEE 802.16a standard, especially the uplink channel specifications. And we gave a brief treatment of the difficulty in uplink channel estimation. In recent years, channel estimation for OFDM systems has received much attention and is the subject of many research papers. Many studies on OFDM channel estimation are based on minimum mean square error criterion. Some optimal MMSE channel estimators have been proposed and completely derived in [5] and [6]. But there is a common problem among them. All of them require the second order statistics of the channel. In other words, we should estimate the statistical characteristic of the channel in advance or continuously. This leads to a complexity problem in addition to the problem of time-variation of the channels.

An alternative way is to use linear or higher order interpolation. This is a quite intuitive method. But linear interpolation works under the condition of strong correlation between pilots and the estimated subcarrier locations. If the pilot spacing is too large, then the estimated subcarrier response may be very different from the true one. In other words, the variation between adjacent pilots cannot be modeled

well by a straight line or higher order polynomials in this case.

Now we are interested in whether there exists a function which can describe the variation between any two adjacent pilots. The answer appears to be yes. We know that the frequency response is transformed from time domain impulse response via the discrete Fourier transform matrix. A related estimator has been proposed in [8], which is called transform-domain estimator. Physically, the idea is roughly similar to upsampling, but is achieved though a different way. Under the assumption of equal pilot spacing, channel gain at pilot locations can be viewed as the downsampled version of the frequency response. In upsampling, it adopts a sinc function for interpolation. However, in tranform-domain processing, it uses IDFT, whose size is equal the number of pilot carriers, to transform the downsampled version to time domain. Then zero samples are padded in the "high frequency" region. Finally, an N_{FFT}-point DFT is performed to convert to the frequency domain. Then we get the channel gains at data locations. It deserves to be mentioned that this approach has no requirement for the statistical properties of the channel compared with MMSE estimator. In this thesis, we start from this concept to develop a suitable estimator for the IEEE 802.16a standard.

3.1 Channel Model

First of all, we should construct a suitable channel model close to real world. Assume that the signal is transmitted over a multipath Rayleigh fading channel characterized by

$$h(\tau, t) = \sum_{l=0}^{L-1} h_l(t)\delta(\tau - \tau_l), \tag{3.1}$$

where the amplitueds $h_l(t)$ are complex valued with Jakes' power spectrum, τ_l is the time delay of the lth path and L is the number of total paths. In addition, the paths are independent from each other. In large cell with high base station, the

multipath channel can be modeled by a few dominant paths, typically 2–6 [9]. For simplicity, we assume path complex gain $h_l(t)$ to be time-invariant over an OFDM symbol time duration. Then the channel model under block fading is given by

$$h(\tau) = \sum_{l=0}^{L-1} h_l \delta(\tau - \tau_l). \tag{3.2}$$

Then we can get $H(e^{j2\pi f})$ by Fourier transform. However, we only concern about the sampling points of $H(e^{j2\pi f})$, which is $H(e^{j2\pi k\Delta f})$ for $k = -N_{FFT}/2+1, \cdots, N_{FFT}/2$, where Δf represents carrier spacing which is equal the inverse of useful symbol time T_b. Then the system can be transformed to discrete time model. The discrete time channel will be

$$\begin{aligned} h'_m &= \frac{1}{N_{FFT}} \sum_{k=-N_{FFT}/2+1}^{N_{FFT}/2} H(e^{j2\pi k\Delta f}) \cdot e^{j\frac{2\pi km}{N_{FFT}}} \\ &= \frac{1}{N_{FFT}} \sum_{k=-N_{FFT}/2+1}^{N_{FFT}/2} \int_0^{T_b} \sum_{l=0}^{L-1} h_l \delta(\tau - \tau_l) \cdot e^{-j2\pi k\Delta f \tau_l} \, d\tau \cdot e^{j\frac{2\pi km}{N_{FFT}}}, \end{aligned}$$

Now we interchange the order of the two summation operators to obtain

$$\begin{aligned} h'_m &= \frac{1}{N_{FFT}} \sum_{l=0}^{L-1} h_l \cdot \sum_{k=-N_{FFT}/2+1}^{N_{FFT}/2} e^{-j2\pi k\Delta f \tau_l} \cdot e^{j\frac{2\pi km}{N_{FFT}}} \\ &= \frac{1}{N_{FFT}} \sum_{l=0}^{L-1} h_l \cdot \frac{e^{-j2\pi(\Delta f\tau_l - \frac{m}{N_{FFT}})(-\frac{N_{FFT}}{2}+1)} - e^{-j2\pi(\Delta f\tau_l - \frac{m}{N_{FFT}})(\frac{N_{FFT}}{2}+1)}}{1 - e^{-j2\pi(\Delta f\tau_l - \frac{m}{N_{FFT}})}} \\ &= \frac{1}{N_{FFT}} \sum_{l=0}^{L-1} h_l \cdot \frac{e^{-j2\pi(\Delta f\tau_l - \frac{m}{N_{FFT}})}}{e^{-\pi(\Delta f\tau_l - \frac{m}{N_{FFT}})}} \cdot \frac{e^{-j2\pi(\Delta f\tau_l - \frac{m}{N_{FFT}})(-\frac{N_{FFT}}{2})} - e^{-j2\pi(\Delta f\tau_l - \frac{m}{N_{FFT}})(\frac{N_{FFT}}{2})}}{e^{j\pi(\Delta f\tau_l - \frac{m}{N_{FFT}})} - e^{-j\pi(\Delta f\tau_l - \frac{m}{N_{FFT}})}} \\ &= \frac{1}{N_{FFT}} \sum_{l=0}^{L-1} h_l \cdot e^{-j\pi(\Delta f\tau_l - \frac{m}{N_{FFT}})} \cdot \frac{2\sin(\pi(\Delta f\tau_l N_{FFT} - m)}{2\sin(\pi(\Delta f\tau_l - \frac{m}{N_{FFT}})}. \end{aligned}$$

If τ_l is a multiple of sampling time T, then all the energy from the lth path concenrate to $h'_{\frac{\tau_l}{T}}$. If not, then the leakage energy to other taps follows the above equation. This phenomenon can be explained from the view point of sampling theorem. A continuous-time signal can be completely represented by its equal-spaced samples under a certain condition. The condtion is that this signal is bandlimited and its

maximum bandwidth is less than one-half the Nyquist rate $\frac{1}{T}$ where T is sampling time. So we need to limit the maximum bandwidth by an ideal lowpass filter. Hence, this leads to a sinc function to convolve with the original signal. If τ_l is a multiple of sampling time, then we sample nothing except the point τ_l after convolution. If not, than we will have nonzero values at other sampling locations.

Hence for the case of sample spaced delays, i.e., $\{\tau_l\}$ are all multiples of T, the delay spread is determined by the longest delay among $\{\tau_l\}$. On the other hand, for non-sample spaced delays, the multipaths are dispersed in the discrete time model. We call this phenomenon "channel spreading."

3.2 The Issue of Transform-Domain Processing

The transform-domain processing proposed in [8] is applicable to either fast- or slowly-fading wireless channels because it inserts pilot carriers into each OFDM symbol to deal with the time-variant channel. And no knowledge of the statistics of the channel is needed.

Nevertheless, the same problem as mentioned in section 2.5 also appears, which is the problem of too few pilots. In sampling theorem, the sampling rate must be larger than the bandwidth of the signal for reconstructing the original signal. If not, an aliasing will occur and distort the value on non-pilot locations. Note that the sampling operation is performed in the frequency domain. So the bandwidth actually means the delay spread of the channel in our problem. For perfectly reconstructing the frequency response, the number of pilot carriers M, i.e., sampling rate, must be larger than the longest delay tap based on transform-domain processing. The result above is suitable for sample spaced delays. Moreover, the situation will be more serious for non-sample spaced delays. Even though there may only be a few paths and the longest delay time is less than $M \cdot T$, transform domain estimator still does

not work for the sake of channel spreading as discussed in the previous section.

In the IEEE 802.16a OFDMA uplink, there are only 5 pilot carriers within a subchannel to estimate the communication channel. And we are not sure whether the actual delay time is a multiple of sampling time or not. Even if the anwser is yes, the channel which can be estimated has a restriction on the delay spread as being less than $5T$. The value is 0.5 μs according to our implementation parameters shown in Table 2.1. Physically, the delay spread in wireless environment is in the range of 5–7 μs, as shown in Table 2.3.

To start, assume that we know the delay time in advance. Under this assumption, as long as the delay spread does not exceed the guard time T_g, the channel can be estimated. Even if τ_l is not a multiple of sampling time, it does not matter. Hence, the channel gain H_{k_i} on pilot carrier k_i can be shown as

$$H_{k_i} = \sum_{l=0}^{L-1} h_l \cdot e^{-j\frac{2\pi k_i \tau_l}{T_b}}, \quad \text{for } i = 0, 1, \cdots, M-1 \ , \tag{3.3}$$

where $k_i \in \{\text{pilot carrier set}\}$ and h_l is complex gain of the lth path. We assume that $\{\tau_l\}$ are known by the receiver. Then the equation above can be viewed as a system of linear equations. Rewriting the form in matrix notation, we get

$$\mathbf{H}_p = \mathbf{F}_p \mathbf{h} \tag{3.4}$$

where $\mathbf{H}_p$ is an $M \times 1$ column vector and $\mathbf{F}_p$ is an $M \times L$ transform matrix with $F_p^{i,l} = e^{-j\frac{2\pi k_i \tau_l}{T_b}}$.

Up to now, the original problem have been split into two parts. One is how to accurately estimate fading channel with the multipath time delays information. The other is how to efficiently track the multipath time delays. Hence, we separately introduce the two parts.We note that this concept is derived from [9]. It estimates the time delays and complex gains of the paths, separately. This estimator assumes that the time delays are slowly time-varying compared with the amplitude and

relative phase of each path. It proposes an interpath interference cancellation delay locked loop to track the channel multipath time delay. Then it adopts MMSE estimator, modified from [5], to estimate the wireless communication channel.

3.3 Multi-Stage Channel Estimator with the Multipath Time Delays Information

In (3.4), we have M equations in L unknown variables. If the number of equations M is less than the number of unknown variabes L then the solution is not unique. Hence, if we attempt to estimate channel successfully, then the number of paths L should be less than the number of pilots M. Consequently, under the condition of $M > L$, we can get the exact solution by solving the system of linear equations (3.4). Unfortunately, we cannot get exact channel gain $\mathbf{H}_p$. We just have the received pilot signal, $\mathbf{Y}_p$, with unkown complex zero-mean Gussian noise:

$$\begin{aligned} \mathbf{Y}_p &= \mathbf{X}_p\mathbf{H}_p + \mathbf{N}_p \\ &= \mathbf{X}_p\mathbf{F}_p\mathbf{h} + \mathbf{N}_p \end{aligned}$$

where $\mathbf{X}_p$ is a diagonal matrix containing the known data on pilot carriers. Removing the pilot modulation on the received symbol, we get the estimate $\widehat{\mathbf{H}}_p$ as

$$\begin{aligned} \widehat{\mathbf{H}}_p &= \mathbf{X}_p^{-1}\mathbf{Y}_p \\ &= \mathbf{F}_p\mathbf{h} + \mathbf{X}_p^{-1}\mathbf{N}_p. \end{aligned}$$

Due to noise perturbation, the vector $\widehat{\mathbf{H}}_p$ is not in the image of $\mathbf{F}_p$. However, We still try to find a vector $\widehat{\mathbf{h}}_{ls}$ such that $\mathbf{F}_p\widehat{\mathbf{h}}_{ls}$ is as close as possible to $\widehat{\mathbf{H}}_p$. That is, we try to minimize the error $\|\widehat{\mathbf{H}}_p - \mathbf{F}_p\widehat{\mathbf{h}}_{ls}\|^2$. We use "$ls$" as shorthand for "least squares solution" which reflects the fact that we are minimizing the sum of the squares of the components of the error:

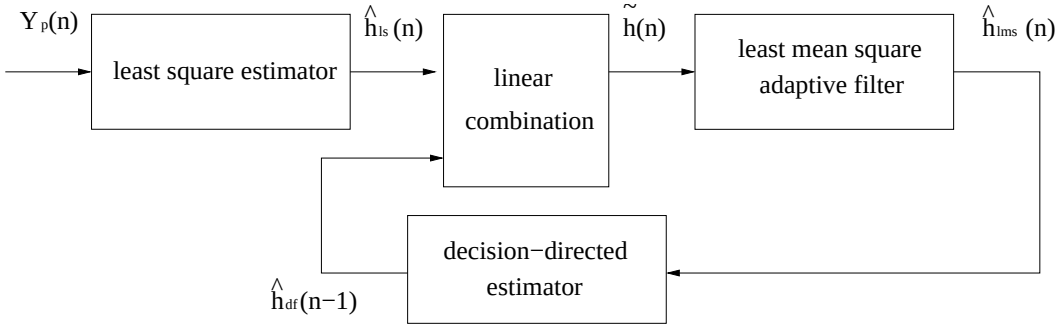

Figure 3.1: Block diagram of the proposed estimator.

$$\begin{aligned}\xi &\overset{\text{def}}{=} \|\widehat{\mathbf{H}}_p - \mathbf{F}_p\widehat{\mathbf{h}}_{ls}\|^2 = (\widehat{\mathbf{H}}_p - \mathbf{F}_p\widehat{\mathbf{h}}_{ls})^H(\widehat{\mathbf{H}}_p - \mathbf{F}_p\widehat{\mathbf{h}}_{ls}) \\ &= \widehat{\mathbf{H}}_p^H\widehat{\mathbf{H}}_p - \widehat{\mathbf{h}}_{ls}^H\mathbf{F}_p^H\widehat{\mathbf{H}}_p - \widehat{\mathbf{H}}_p^H\mathbf{F}_p\widehat{\mathbf{h}}_{ls} + \widehat{\mathbf{h}}_{ls}^H\mathbf{F}_p^H\mathbf{F}_p\widehat{\mathbf{h}}_{ls}.\end{aligned}$$

Minimizing ξ to find $\widehat{\mathbf{h}}_{ls}$, we take the partial derivative as

$$\nabla_{\widehat{\mathbf{h}}_{ls}}\xi = 2\mathbf{F}_p^H\mathbf{F}_p\widehat{\mathbf{h}}_{ls} - 2\mathbf{F}_p^H\widehat{\mathbf{H}}_p = \mathbf{0}.$$

Then we get

$$\widehat{\mathbf{h}}_{ls} = (\mathbf{F}_p^H\mathbf{F}_p)^{-1}\mathbf{F}_p^H\widehat{\mathbf{H}}_p. \tag{3.5}$$

Note that the vector $\mathbf{F}_p\widehat{\mathbf{h}}_{ls}$ is the projection of $\widehat{\mathbf{H}}_p$ to the image of $\mathbf{F}_p$. And the vector $\left(\widehat{\mathbf{H}}_p - \mathbf{F}_p\widehat{\mathbf{h}}_{ls}\right)$ is perpendicular to the image of $\mathbf{F}_p$. In addtion, with more pilots, then we can get more accurate estimate $\widehat{\mathbf{h}}_{ls}$ for real complex gain $\mathbf{h}$. That is because the noise terms have been averaged among those equations. However, the number of pilot carriers is about the number of paths in our case. As expected, the performace is not good, if we only use the least square approximation. Hence, we will introduce more methods to improve the performance in following subsections. The block diagram of the proposed estimator is shown in Fig. 3.1.

3.3.1 Optimally Combining Decision-Directed and Least Squares Channel Estimators

We want to improve the performance of least square estimator. Note that the complex gain of each path is a continuous function of time in real world. There

is no abrupt change in the channel response during a short duration. That is the channel at the moment is similar to that at next time. We can use the correlation of the channel between adjacent symbols to enhance the accuracy of the channel estimate. Hence, we adopt decision-directed estimator to bring the information of previous channel, and combine least square channel estimator to extract more information. Firstly, we have, at time n,

$$\begin{aligned}
\widehat{\mathbf{H}}_{ls} &= \mathbf{F}\widehat{\mathbf{h}}_{ls} \\
&= \mathbf{F}(\mathbf{F}_p^H\mathbf{F}_p)^{-1}\mathbf{F}_p^H\widehat{\mathbf{H}}_p \\
&= \mathbf{F}(\mathbf{F}_p^H\mathbf{F}_p)^{-1}\mathbf{F}_p^H(\mathbf{F}_p\mathbf{h}+\mathbf{X}_p^{-1}\mathbf{N}_p) \\
&= \mathbf{F}\mathbf{h}+\mathbf{F}(\mathbf{F}_p^H\mathbf{F}_p)^{-1}\mathbf{F}_p^H\mathbf{X}_p^{-1}\mathbf{N}_p \\
&= \mathbf{F}\mathbf{h}+\widetilde{\mathbf{N}}
\end{aligned}$$

where $\mathbf{F}$ is a $K \times L$ transform matrix with $F^{i,j} = e^{-j\frac{2\pi k_i \tau_j}{T_b}}$ and

$$\widetilde{\mathbf{N}} = \mathbf{F}(\mathbf{F}_p^H\mathbf{F}_p)^{-1}\mathbf{F}_p^H\mathbf{X}_p^{-1}\mathbf{N}_p.$$

If X_{k_i} is transmitted data on carrier k_i and the receiver decision for X_{k_i} is $\widehat{X}_{k_i}$, then the decision-directed channel gain estimate is

$$\widehat{H}_{df,k_i} = H_{k_i} + \frac{\Delta X_{k_i} H_{k_i}}{\widehat{X}_{k_i}} + \Delta H_{k_i} + \frac{N_{k_i}}{\widehat{X}_{k_i}}, \quad \text{for } i = 0, 1, \cdots, K-1 \qquad (3.6)$$

where $k_i \in \{\text{subcarrier set within a subchannel}\}$ and $\Delta X_{k_i} = X_{k_i} - \widehat{X}_{k_i}$ is the decision error with decision error probability symbol error rate and ΔH_{k_i} is a difference by the time for the sake of channel variation. Eq. (3.6) has been modified from [10] by adding the term of ΔH_{k_i} in order to be applicable to time-variant channels. The term ΔH_{k_i} becomes more significant in high SNR. Under the assumption of slowly-time variant channel, we use linear combination between two estimators so as to suppress the noise term, where the decision feedback estimator brings in the channel information at the previous symbol:

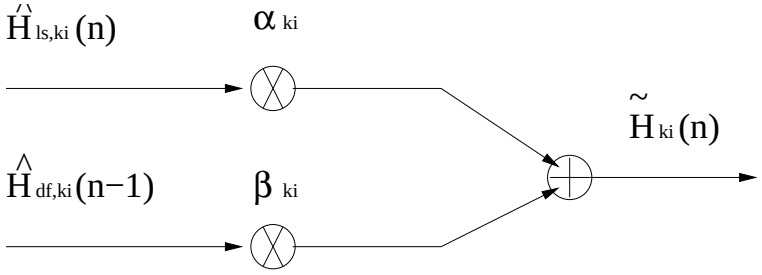

Figure 3.2: Linear combining in frequency domain.

$$\widetilde{H}_{k_i}(n) = \alpha_{k_i}\widehat{H}_{ls,k_i}(n) + \beta_{k_i}\widehat{H}_{df,k_i}(n-1). \tag{3.7}$$

For convenience, we drop the subscript k_i and time index n in the following writing. We want to find the optimal weights to approach the actual channel gain. We adopt minimum mean square error approach to minimize $E[|\widetilde{H} - H|^2]$. Taking derivatives with respect to α and β and setting the results to zero, we get

$$\begin{aligned}
\frac{\partial E[(\widetilde{H}-H)(\widetilde{H}-H)^*]}{\partial \alpha} &= E[2(\widetilde{H}-H)\widehat{H}_{ls}^*] = 0, \\
\frac{\partial E[(\widetilde{H}-H)(\widetilde{H}-H)^*]}{\partial \beta} &= E[2(\widetilde{H}-H)\widehat{H}_{df}^*] = 0.
\end{aligned}$$

The exact solutions of α and β are complicated. For symplicity, we assume that $\alpha + \beta \simeq 1$. Then we get

$$\begin{aligned}
\alpha^{-1} &= 1 + \frac{E\left[\widetilde{N}\widetilde{N}^*\right]}{E\left[\Delta X \Delta X^*\right] E\left[HH^*\right] E\left[\frac{1}{XX^*}\right] + E[\Delta H \Delta H^*] + E[NN^*] E\left[\frac{1}{XX^*}\right]} \\
&\quad + \frac{E\left[\widetilde{N}\widetilde{N}^*\right]\left(E\left[\Delta X \Delta X^*\right] E\left[HH^*\right] E\left[\frac{1}{XX^*}\right] + \frac{1}{2}E[\Delta H \Delta H^*] + E[NN^*] E\left[\frac{1}{XX^*}\right]\right)}{E[HH^*]\left(E\left[\Delta X \Delta X^*\right] E\left[HH^*\right] E\left[\frac{1}{XX^*}\right] + E[\Delta H \Delta H^*] + E[NN^*] E\left[\frac{1}{XX^*}\right]\right)}, \\
\beta^{-1} &= 1 + \frac{E\left[\Delta X \Delta X^*\right] E\left[HH^*\right] E\left[\frac{1}{XX^*}\right] + E[\Delta H \Delta H^*] + E[NN^*] E\left[\frac{1}{XX^*}\right]}{E\left[\widetilde{N}\widetilde{N}^*\right]} \\
&\quad + \frac{E\left[\Delta X \Delta X^*\right] E\left[HH^*\right] E\left[\frac{1}{XX^*}\right] + \frac{1}{2}E[\Delta H \Delta H^*] + E[NN^*] E\left[\frac{1}{XX^*}\right]}{E[HH^*]}.
\end{aligned} \tag{3.8}$$

Note that the second right-hand term in each equation is the ratio of interference part, and the third term is the ratio of each interference part to the squared norm of the channel gain.

Suppose that decision errors take place mostly between adjacent constellation points which have the minimum distance d, then we can approximate $E\left[\Delta X \Delta X^*\right] \simeq d^2\text{SER}$. Assuming equal probability on all constellation points, we can compute the term $E\left[\frac{1}{XX^*}\right]$. Furthermore, $E[HH^*]$ can be written in terms of $\mathbf{h}$ as

$$E[H_{k_i}H_{k_i}^*] = E\left[\left\|\sum_j F^{i,j}h_j\right\|^2\right].$$

Because $\{h_j\}$ are mutually independent, we can simplify the above equation as

$$E[H_{k_i}H_{k_i}^*] = \sum_j \left\|F^{i,j}\right\|^2 E\left[h_j h_j^*\right].$$

Additionally, $F^{i,j}$ is in the form of $e^{-j\frac{2\pi k_i \tau_j}{T_b}}$. Hence, the norm of $F^{i,j}$ is 1 for all i, j. Thus

$$E[H_{k_i}H_{k_i}^*] = \sum_j E\left[h_j h_j^*\right], \quad i = 0, \cdots, K-1. \tag{3.9}$$

Hence we can estimate $E[H_{k_i}H_{k_i}^*]$ by averaging the received power.

Similarly, $E[\Delta H \Delta H^*]$ can be rewritten as

$$\begin{aligned}
E[\Delta H_{k_i}\Delta H_{k_i}^*] &= E\left[\left\|H_{k_i}(n) - H_{k_i}(n-1)\right\|^2\right] \\
&= E\left[\left\|\sum_j F_{i,j}\left(h_j(n) - h_j(n-1)\right)\right\|^2\right] \\
&= \sum_j \left\|F^{i,j}\right\|^2 E\left[(h_j(n) - h_j(n-1))(h_j(n) - h_j(n-1))^*\right] \\
&= \sum_j E\left[(h_j(n) - h_j(n-1))(h_j(n) - h_j(n-1))^*\right]
\end{aligned}$$

where $\{h_j\}$ is modeled as Rayleigh distribution with Jakes' power spectrum and n is the time index. To further simplify the above equation, note that

$$E\left[(h_j(n) - h_j(n-1))(h_j(n) - h_j(n-1))^*\right] = 2E[h_j h_j^*](1 - J_0(2\pi f_d T_s)).$$

Then we get

$$E[\Delta H_{k_i}\Delta H_{k_i}^*] = 2(1 - J_0(2\pi f_d T_s))\left(\sum_j E[h_j h_j^*]\right), \quad i = 0, \cdots, K-1 \tag{3.10}$$

Moreover, assume the noise term $E[NN^*]$ is known or has been estimated. Then we can rewrite $E\left[\widetilde{N}\widetilde{N}^*\right]$ in terms of $E[NN^*]$ as

$$\begin{aligned} E\left[\widetilde{N}_{k_i}\widetilde{N}^*_{k_i}\right] &= \sum_{j=0}^{L-1} Q^{i,j} E\left[\frac{N_{p,j}N^*_{p,j}}{X_{p,j}X^*_{p,j}}\right] \\ &= \sum_{j=0}^{L-1} Q^{i,j} E\left[N_{p,j}N^*_{p,j}\right] E\left[\frac{1}{X_{p,j}X^*_{p,j}}\right], \qquad i = 0, \cdots, K-1, \end{aligned} \tag{3.11}$$

where $\mathbf{Q} = \mathbf{F}(\mathbf{F}_p^H\mathbf{F}_p)^{-1}\mathbf{F}_p^H$ and $Q^{i,j}$ is an element in $\mathbf{Q}$. Finally, substituting in the known values, we can find the best weight α and β.

Note that we should find α_{k_i} and β_{k_i} for each subcarrier k_i within the subchannel. We can consider to take average in each path instead of each subcarrier, because the number of paths is smaller than the number of subcarriers within the subchannel. Then we rewrite (3.6) and transform it to time domain as

$$\begin{aligned} \widehat{\mathbf{h}}_{df} &= (\mathbf{F}^H\mathbf{F})^{-1}\mathbf{F}^H\widehat{\mathbf{H}} \\ &= (\mathbf{F}^H\mathbf{F})^{-1}\mathbf{F}^H(\mathbf{H} + \mathbf{\Delta_H} + \mathbf{\Delta_X}\mathbf{H} + \mathbf{X}^{-1}\mathbf{N}) \\ &= \mathbf{h} + \mathbf{\Delta_h} + (\mathbf{F}^H\mathbf{F})^{-1}\mathbf{F}^H(\mathbf{\Delta_X}\mathbf{H} + \mathbf{X}^{-1}\mathbf{N}) \end{aligned} \tag{3.12}$$

where $\mathbf{\Delta_h} = [\Delta h_0, \cdots, \Delta h_{L-1}]^\top$ and $\mathbf{\Delta_X}$ is a diagonal matrix containing the element $\frac{\Delta X_i}{X_i}$. For a path, we have

$$\widehat{h}_{ls,l} = h_l + \delta_l, \quad \widehat{h}_{df,l} = h_l + \Delta h_l + \epsilon_l + \varepsilon_l, \tag{3.13}$$

where

δ_l is the lth element in $(\mathbf{F}_p^H\mathbf{F}_p)^{-1}\mathbf{F}_p^H\mathbf{X}_p^{-1}\mathbf{N}_p$,

ϵ_l is the lth element in $(\mathbf{F}^H\mathbf{F})^{-1}\mathbf{F}^H\mathbf{\Delta_X}\mathbf{H}$, and

ε_l is the lth element in $(\mathbf{F}^H\mathbf{F})^{-1}\mathbf{F}^H\mathbf{X}^{-1}\mathbf{N}$.

Applying linear combination in each path, we obtain a refined estimate as

$$\widetilde{h}_l = \alpha_l\widehat{h}_{ls,l} + \beta_l\widehat{h}_{df,l}. \tag{3.14}$$

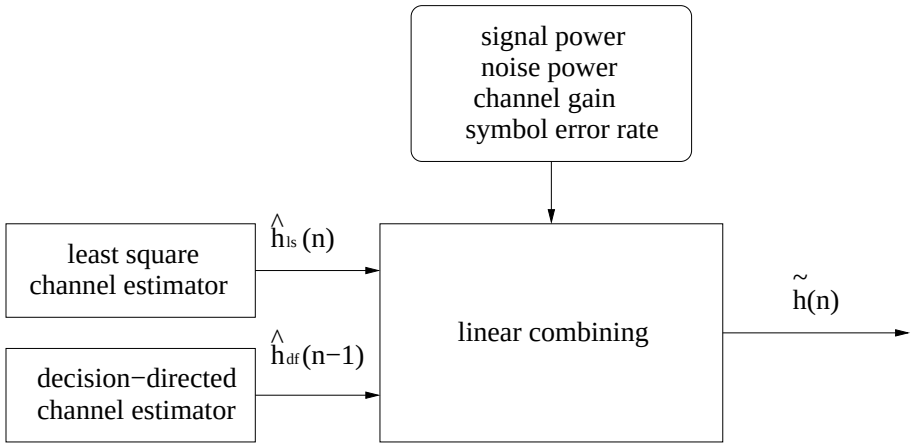

Figure 3.3: Combined decision-directed and least square channel estimator.

Following the same procedure as above, we can get the expressions for α_l and β_l similar to (3.8) as

$$\begin{aligned}
\alpha^{-1} &= 1 + \frac{E\left[\delta\delta^*\right]}{E\left[\epsilon\epsilon^*\right] + E\left[\varepsilon\varepsilon^*\right] + E[\Delta h \Delta h^*]} \\
&\quad + \frac{E\left[\delta\delta^*\right]\left(E\left[\epsilon\epsilon^*\right] + E\left[\varepsilon\varepsilon^*\right] + \frac{1}{2}E[\Delta h \Delta h^*]\right)}{E[hh^*]\left(E\left[\epsilon\epsilon^*\right] + E\left[\varepsilon\varepsilon^*\right] + E[\Delta h \Delta h^*]\right)}, \\
\beta^{-1} &= 1 + \frac{E\left[\epsilon\epsilon^*\right] + E\left[\varepsilon\varepsilon^*\right] + E[\Delta h \Delta h^*]}{E\left[\delta\delta^*\right]} \\
&\quad + \frac{\left(E\left[\epsilon\epsilon^*\right] + E\left[\varepsilon\varepsilon^*\right] + \frac{1}{2}E[\Delta h \Delta h^*]\right)}{E[hh^*]}.
\end{aligned} \tag{3.15}$$

The block diagram is shown in Fig. 3.3.

3.3.2 Least Mean Square Adaptation

There is a little improvement of performance by combining decision-directed and least square channel estimator. But it is not enough. The compound estimator still needs high SNR to achieve sufficiently low symbol error rate. We need much more improvement in practice. Hence, we take more adjacent symbols into account in hope for more improvement. We expect there exists a perfect system whose input and output are respectively the result of (3.14), $\widetilde{h}_l(n)$, and the complex gain of lth path, $h_l(n)$. For simplicity, we assume the system is a finite impulse response filter.

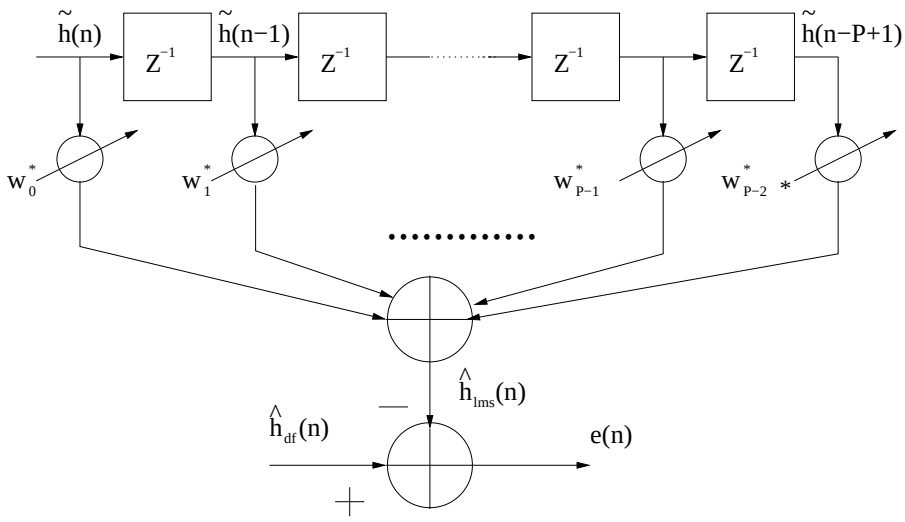

Figure 3.4: The structure of a P-tap transversal adaptive filter.

The block diagram of the system is illustrated in Fig. 3.4. Then we need to get the parameters of the system, i.e., the value of the weights. Since the channel is time-variant, the weights are not fixed. Adaptive filters, by their very nature, are self-designing systems which can adjust themselves to different environments. Hence we adopt P-tap transversal adaptive filter. Each path $\widetilde{h}_l(n)$ has its own adaptive filter. Since the concept is the same, we just pick one to explain without suffix l. Then we can express the above system as

$$\widehat{h}_{lms}(n) \;=\; \sum_{i=0}^{P-1} w_i(n)^* \widetilde{h}(n-i) \tag{3.16}$$

where $w_i(n)$ is the ith tap weight at time n and $\widehat{h}_{lms}(n)$ is the output which is the esimate of $h(n)$. In matrix notation, we have

$$\widehat{h}_{lms}(n) \;=\; \mathbf{w}(n)^T \widetilde{\mathbf{h}}(n)$$

where the tap-weight vector $\mathbf{w}(n) = [w_0^*(n)\ w_1^*(n)\ \cdots\ w_{P-1}^*(n)]^T$ and the filter input vector $\widetilde{\mathbf{h}}(n) = [\widetilde{h}(n)\ \widetilde{h}(n-1)\ \cdots\ \widetilde{h}(n-P+1)]^T$.

In order to minimize the estimation error $e(n) = h(n) - \widehat{h}_{lms}(n)$, the tap weights

$w_i(n)$ should be carefully chosen at each time. The mean-square error is given by

$$\begin{aligned}\xi &= E\left[\|e(n)\|^2\right] = E\left[\|h(n) - \widehat{h}_{lms}(n)\|^2\right] \\ &= E\left[\left\| h(n) - \sum_{i=0}^{P-1} w_i(n)^* \widetilde{h}(n-i) \right\|^2\right]. \end{aligned} \tag{3.17}$$

Under the assumption of the performance surface is convex, then the minimum point exists. Hence we can use iterative method to search for its minimum point to find the optimal tap weights. Firstly, we guess a likely point on the performance surface and take a small step in the direction in which the cost function decreases fastest. Since the exact ξ is hard to get, then it is simply replaced by its instantaneous coarse estimate $\|e(n)\|^2$. Hence the update equation in LMS algorithm is shown as below

$$\mathbf{w}(n+1) = \mathbf{w}(n) + 2\mu e^*(n)\widetilde{\mathbf{h}}(n). \tag{3.18}$$

where μ is the step size. The update approach is known as the method of steepest descent. There exists another update method, such as Newton' method. We can say that the weight update equation is the core in LMS algorithm. When update method is decided, the state of convergence have been roughly determined.

Furthermore, the step size μ also affect the speed of convergence. With larger step size, the $\mathbf{w}$ converges quickly. But if a wrong step size is picked, it may be lead to unstable. For the stability of the LMS algorithm, the following inequality must be held.

$$\mu \leq \frac{1}{3\mathrm{tr}[\mathbf{R}]} = \mu_{max}$$

where $\mathbf{R} = E\left[\widetilde{\mathbf{h}}(n)\widetilde{\mathbf{h}}^H(n)\right]$. The term of $\mathrm{tr}[\mathbf{R}]$ can be further simplified as

$$\begin{aligned}\mathrm{tr}[\mathbf{R}] &= \sum_{i=0}^{P-1} E\left[h(n-i)h(n-i)^*\right] \\ &= \sum_{i=0}^{P-1} E\left[\|h(n)\|^2\right] \\ &= P \cdot E\left[\|h(n)\|^2\right]. \end{aligned}$$

Then we can get the range of μ for stability

$$\mu \leq \frac{1}{3PE\left[\|h(n)\|^2\right]}. \tag{3.19}$$

Since the mobile communication system operates under time-variant channel, the optimal weights are also time-variant. If too small step size is selected, then it is impossible to approach the optimal weights successfully. Hence, we consider a larger step size.

There is another question for implementation. That is how many taps we choose to design the adaptive filter. In general, the more taps we use, the better performance we achieve. But the enhancement margin of performance will decrease as the more taps we use. In other words, those symbols too far back have no use in estimating the complex gain $h(n)$. We only need to adequate number of taps, then the computation complexity can be reduced. Hence we should take the coherent time into account. The channel approximately remains the same during the coherent time. Furthermore, the coherent time T_c is related to the Duppler shift f_d approximately as

$$T_c \approx \frac{1}{f_d} = \frac{c}{vf_c}$$

where c is velocity of light, v is vehicle velocity, and f_c is carrier frequency. We cannot find the adequate number P only from the coherent time T_c. A more useful factor is the ratio of coherent time T_c to symbol duration T_s. The adequate number should be around the ratio.

It may be argued that we do not know the desired output $h(n)$. Then how do we compute the error term $e(n)$ to update the weights? A technique to overcome this problem is to use the decision directed estimate $\widehat{h}_{df}(n)$ from (3.12) in replace of $h(n)$. We have discussed in detail about decision-directed approach in subsection 2.3.3. The decision directed estimate $\widehat{h}_{df}(n)$ is not always correct depending on on

the correctness of the detected data. If the communication environment is very bad, then the error probability of the detected data is high. Using wrong decision data to estimate the channel response can lead to more errors. Now, we replace the actual complex gain $h(n)$ with $\widehat{h}_{df}(n)$, the same problem occurs again. However, we can combine the decision-directed approach and least square channel estimators to control the noise effect. Then by using an adaptive filter in the following, the noise power will reach an acceptable level. And the error of decision-directed approach can be decreased to some degree.

3.4 Simulation Results

The simulation parameters are set up according to the IEEE 802.16a standard. The details can be found in subsection 2.4.2. The OFDMA physical layer defines N_{FFT} to be equal to 2048. Usable carriers are divided into subchannels, and each subchannel has 53 subcarriers including 5 pilots and 48 data carriers. The system occupies a transmission bandwidth of 10 MHz and the sampling time T is $\frac{7}{80}$ μs. The length of cyclic prefix T_g is equal to $256T$. Hence the duration of an OFDM symbol is $201\frac{1}{5}$ μs. The channel model is Rayleigh fading and each path is complex valued with Jakes' spectrum and simulated by a sum-of-sinusoids statistical model [13]. We choose a low vehicle speed $V = 26$ km/h, corresponding to $f_dT \approx 0.01$ under the condition of carrier frequency of 2 GHz. The power level and delay of each path are specified in Table 3.1. And each path gain roughly follows the exponential power delay profile. In order to focus on evaluating the performance of the proposed estimator, encoding and interleaving have been omitted in the simulation. In addition, we assume perfect synchronization at the receiver. The adopted constellation is 16QAM which includes both amplitude and phase modulations in order to evaluate our proposed estimator in all its aspects. Note that we just simulate a subchannel used by a subscriber so that there is no interference from other subchannels.

Table 3.1: Characteristics of Simulation Channel A

Tap	Time delay (μs)	Time delay (T)	Average Power (dB)
1	0	0	0
2	0.175	2	-7.2
3	0.35	4	-14.4
4	0.525	6	-21.6
5	0.875	10	-36

3.4.1 Comparison Between the Proposed and the Least Squares Channel Estimators

The mean square error of channel estimation and the uncoded-16QAM symbol error rate are presented in Figs. 3.5 and 3.6, respectively. The estimation error is given by the difference between the estimate value and actual channel response. The simulation assumes that the multipath time delays are known. Note that the horizontal variable used in the figures are the average symbol power to noise power ratio which is 6 dB above E_b/N_0 under the same condition. Compared with the least square estimator, the mean square error in Fig. 3.5 has a great improvement by selecting the proposed estimator. Then there is also an performance enhancement of 7–8 dB in Fig. 3.6. We also plot the curve with complete knowledge of channel gains. That shows the limit which the best channel estimation can achieve. The simulation shows that the performance of the proposed estimator is close to that of the perfect channel estimation.

In the least squares channel estimator, there are only five pilots to estimate the five paths. There is no other information used in this method. And the noise terms in pilot locations will be distributed to the data locations though transform process. In addition, the transform process also enhances the noise power level in data locations than that in pilot locations and brings about channel estimation error. Hence the accuracy of channel estimation in data locations will be degraded.

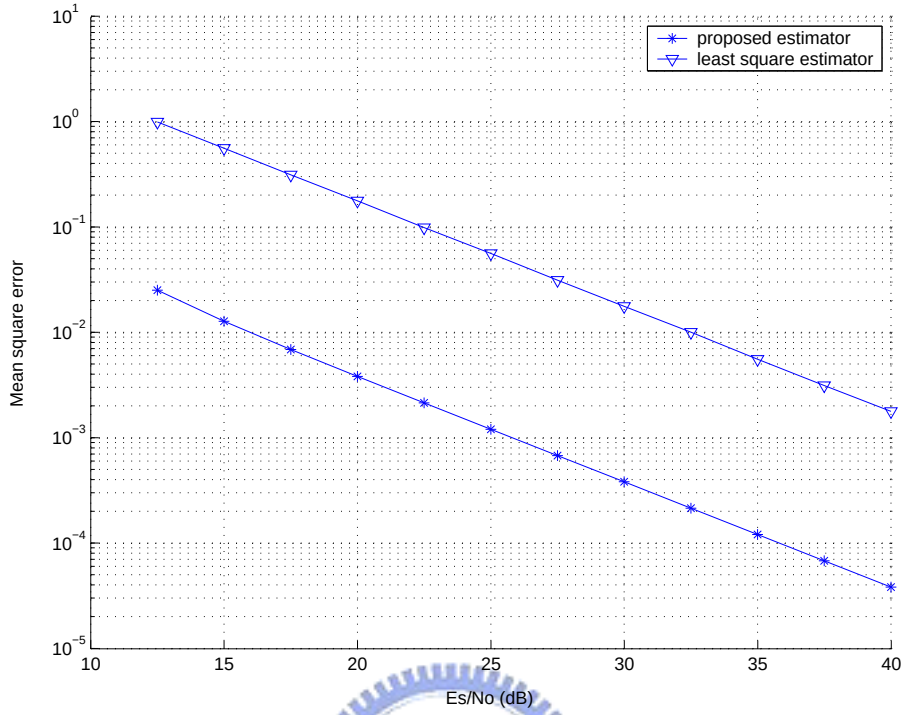

Figure 3.5: Channel estimation MSE of only least squares estimator and proposed estimator.

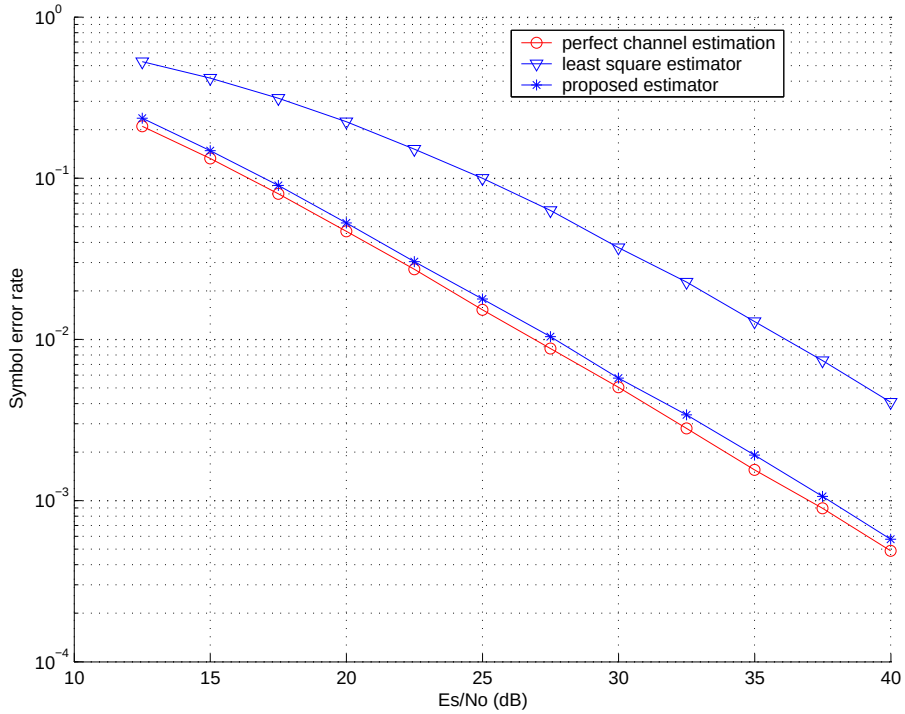

Figure 3.6: Uncoded-16QAM SER performance of only least squares estimator and proposed estimator.

On the other hand, the proposed estimator uses the previous symbols to assist in channel estimation. Since the channel impulse responses continuously vary, we can collect the information of the previous symbols to smooth the estimate of impulse response derived form least squares estimator. At the same time, the noise term is averaged in the smoothing process. Hence the proposed estimator effectively reduces the noise power, and then enhances the accurancy of estimated channel. However the smoothing in frequency domain is not taken into account, because the average carrier spacing within a subchannel, about 200 kHz, is close to the potential coherent bandwidth, about 166 kHz according to delay spread 6–7 μs. Hence the complex gains of adjacent subcarriers are not similar, and we cannot take average among them to reduce noise power.

In addition, we try to find the quantitative relation between mean square error of channel estimation and the symbol error rate. In fact, the mean square error of channel estimation is an average value among overall used subcarriers. Hence, we cannot substitute an average value in Q-function to obtain the theoretical symbol error rate.

The proposed estimator is composed of multi-stages shown in Fig. 3.7. Each stage can be viewed as an independent channel estimator. Then each channel estimator is concatenated together to become a large one. And the performance is improved stage by stage. In order to investigate the performance enhancement of each stage, the simulation is performed by adding each stage step by step. There are four choices of channel impulse response estimates labelled in Fig. 3.7. Then the impulse response is transformed into the frequency response for the sake of demodulation. The performance is shown in Figs. 3.8 and 3.9. One shows mean square error of channel estimation, and the other shows uncoded-16QAM symbol error rate.

The performance of the estimate $\widetilde{h}(n)$ is much better than that of $\widehat{h}_{ls}(n)$ in low SNR. However the improvement in high SNR is not obvious, which is the effect of

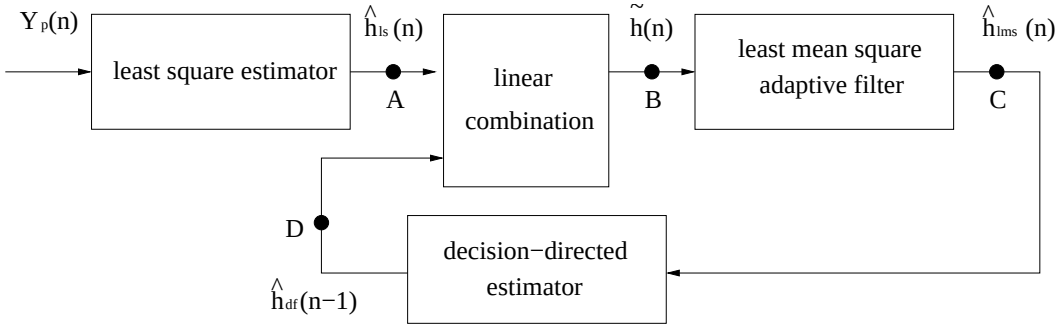

Figure 3.7: Block diagram of the proposed estimator.

$\Delta h(n)$ shown in (3.13) masks the benefit of the linear combination between $\widehat{h}_{ls}(n)$ and $\widehat{h}_{df}(n-1)$. Then the LMS adaptive filter is adopted to trace the time variant channel. It brings the great performance improvement, especially in high SNR. We conjecture that the LMS adaptive filter is the key which quite substantially improves the performance. The decision-directed estimator is used as the final stage. It can further reduce the noise power and achieve more accurate channel estimate. Now we do not have to worry about the effect of error propagation in decision-directed estimator. After the three previous stages, the noise power has been greatly suppressed. Hence, $\widehat{h}_{df}(n)$ has a little more improvement than the estimate $\widehat{h}_{lms}(n)$.

In order to investigate the reliability of the proposed estimator, several kinds of channels are simulated. Two more channels are shown in Tables 3.2 and 3.3.

In Table 3.2, the mutipath time delays $\{\tau_l\}$ are at non-sample spaced positions and the longest delay is about 5 μs. The other features of channel B are the same as that of channel A. The simulation results are shown in Figs. 3.10 and 3.11. The two curves for channel A and channel B are almost overlapping in MSE of the estimated channel response and in SER performance. That means that the proposed estimator is insensitive to the values of time delays under the assumption that time delays are known. And the proposed estimator is not restricted by whether the time delays $\{\tau_l\}$ are sample spaced or non-sample spaced.

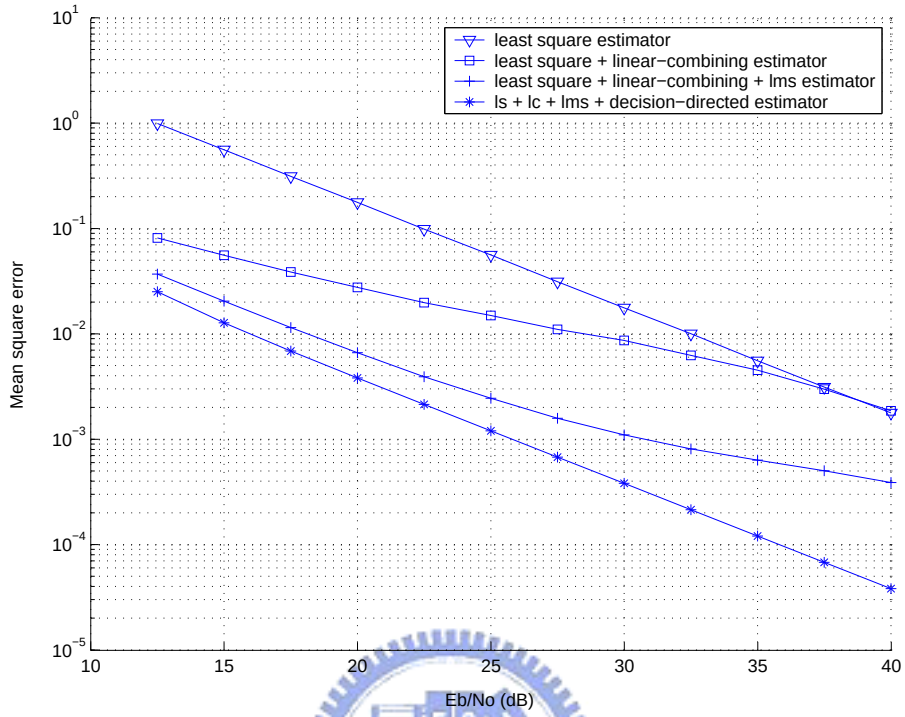

Figure 3.8: Channel estimation MSE of each stage.

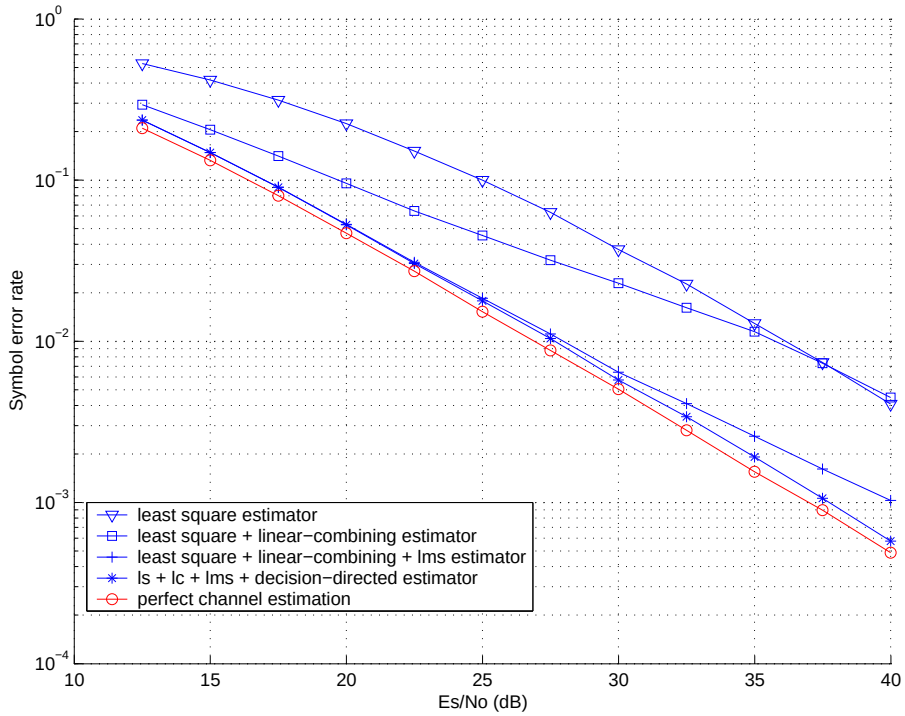

Figure 3.9: Uncode-16QAM SER performance of each stage.

Table 3.2: Characteristics of Simulation Channel B

Tap	Time delay (μs)	Time delay (T)	Average Power (dB)
1	0	0	0
2	0.218 75	2.5	-7.2
3	0.367 5	4.2	-14.4
4	1.4	16	-21.6
5	5.075	58	-36

Table 3.3: Characteristics of Simulation Channel C

Tap	Time delay (μs)	Time delay (T)	Average Power (dB)
1	0	0	-3.23
2	0.175	2	-5.27
3	0.35	4	-7.49
4	0.525	6	-8.46
5	0.875	10	-10.22

In addition, we also test the proposed estimator under different multipath intensity profiles. Note that the multipath intensity profile of of channel C has linear decay instead of exponential decay. The simulation results are also almost the same as channel A shown in Figs. 3.10 and 3.11. That implies the proposed estimator is robust against various power profiles.

3.4.2 Evaluation of the Proposed Estimator under Different Doppler Spreads

In order to verify the performance in various speed conditions, we take different Doppler spreads into account. Simulations are carried out under the same condition except the vehicle speed. Figs. 3.12 and 3.13 show mean square error and symbol error rate respectively. Obviously, we can see that the performance degrades either in symbol error rate or in mean square error, when the Doppler spread increases. That is because the the proposed estimator uses previous estimates in estimation of later channels. And the high vehicle velocity brings about a fast time-variant channel.

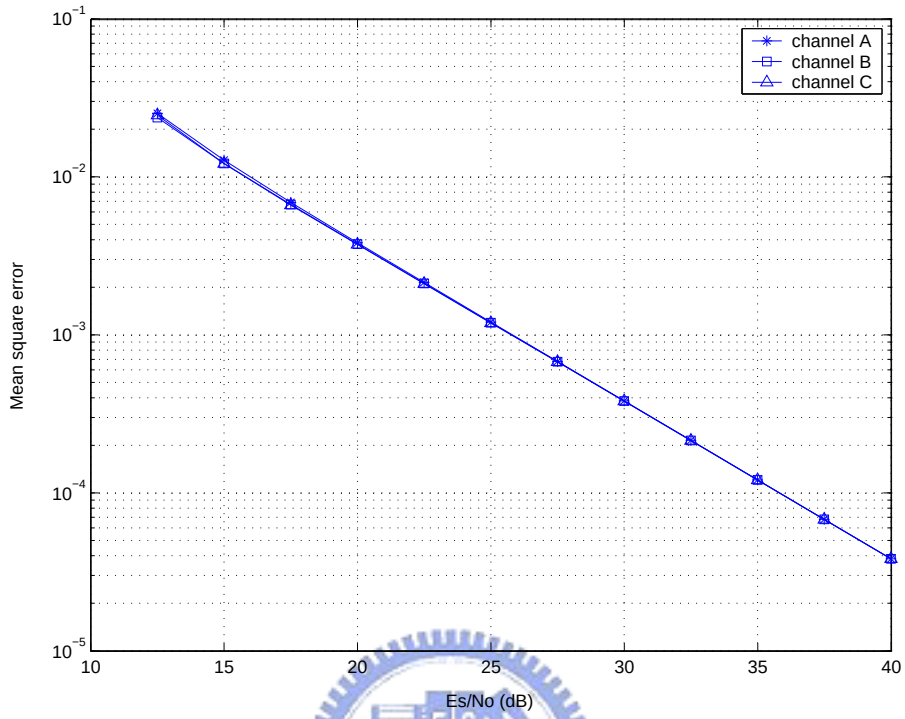

Figure 3.10: Channel estimation MSE under various channel conditions.

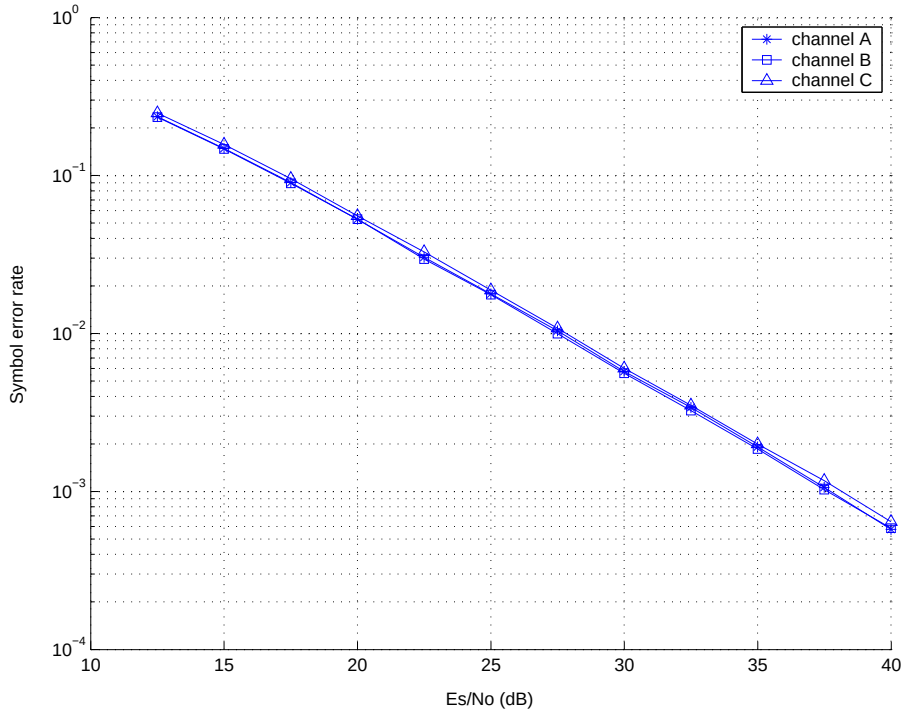

Figure 3.11: Uncoded-16QAM SER performance under various channel conditions.

Then the correlation of the channel between adjacent OFDM symbols decays soon, and the useful information among previous OFDM symbols consequentially reduces. Hence, the symbol error rate and mean square error are worse higher speeds. In other words, the adaptive filter adopted in the proposed estimator is a kind of smoothing process among the estimates along the time axis. Its aim is to average the noise and reduce estimation error. But if the channel varies quickly, then it will induce interference due to channel variation.

We also find that the mean square errors at different speeds merge to one point at high SNR but the symbol error rates do not. This implies that the estimation error cannot be viewed as AWGN noise. It is time-dependent random variable. If the estimation error is large in nth OFDM symbol, then it is probably large at next OFDM symbol, too. This phenomenon is shown in Fig. 3.14. We conjecture that different speeds lead to different time dependent conditions. Hence, even with the same SNR and mean square error, the symbol error rates are still different.

3.4.3 Analysis of Intercarrier Interference

Up to now, the simulation is performed under the assumption that the channel is block fading. That is the channel is stationary during an OFDM symbol period. Then the effect of the intercarrier interference (ICI) does not appear in the results of the simulations. Hence, we release the restriction and make the channel vary at each sample in order to observe the effect of the intercarrier interference. The nth sample of the received signal r_n is then given by

$$r_n = (s * h)_n = \sum_{k=0}^{N_{FFT}-1} s_k h_{n,n-k}$$

where $h_{n,k}$ is the time-variant channel impulse response at sample n and s_k is the kth sample of transmitted signal.

Due to the Doppler spread effect, the power of transmitted data on subcarrier k

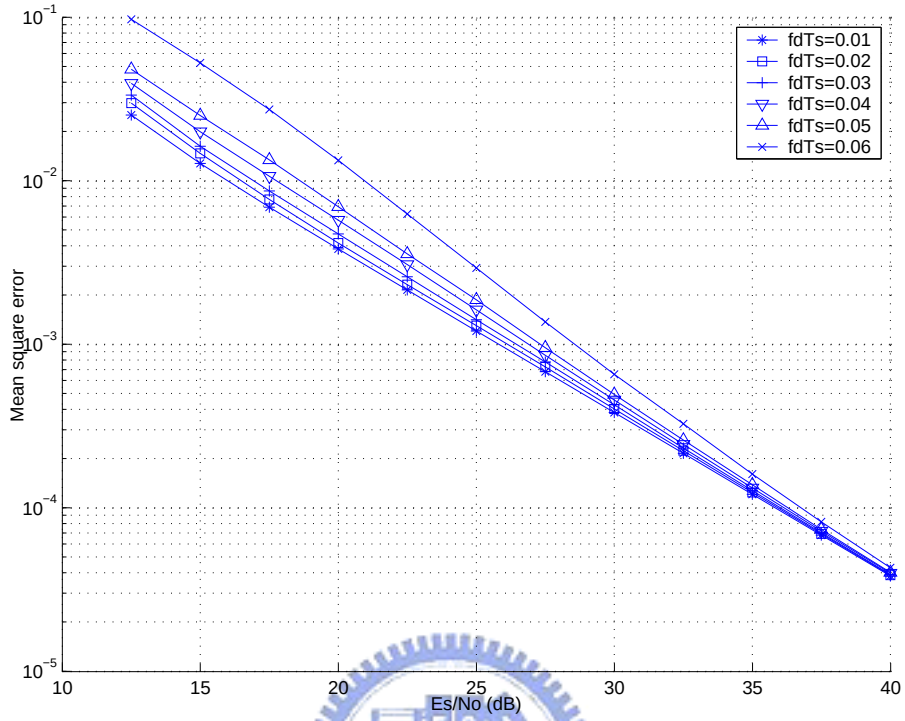

Figure 3.12: Channel estimation MSE under different values of $f_d T_s$.

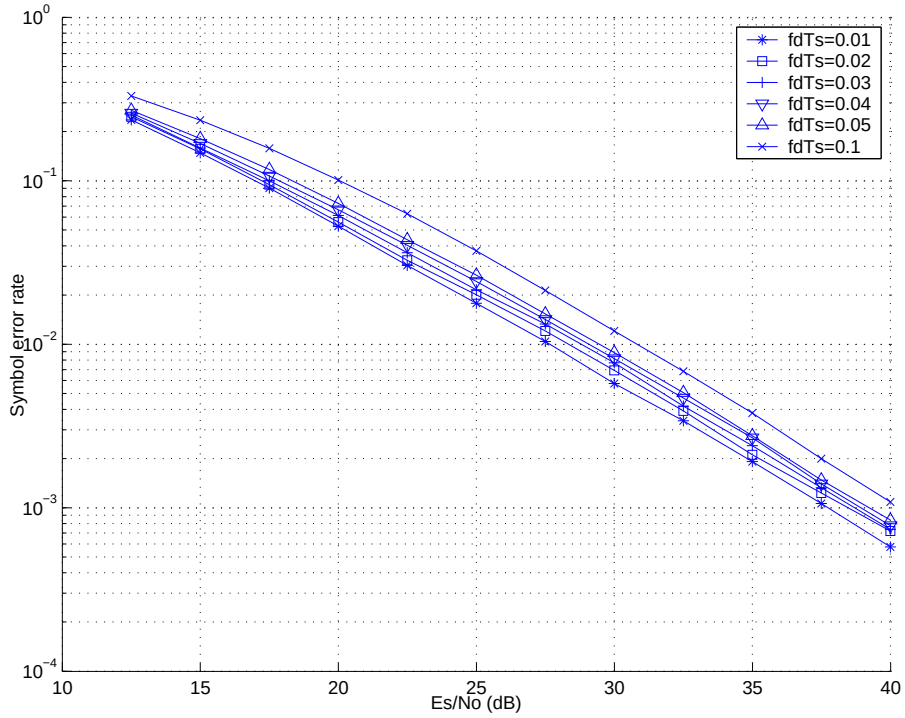

Figure 3.13: Uncoded-16QAM SER performance under different values of $f_d T_s$.

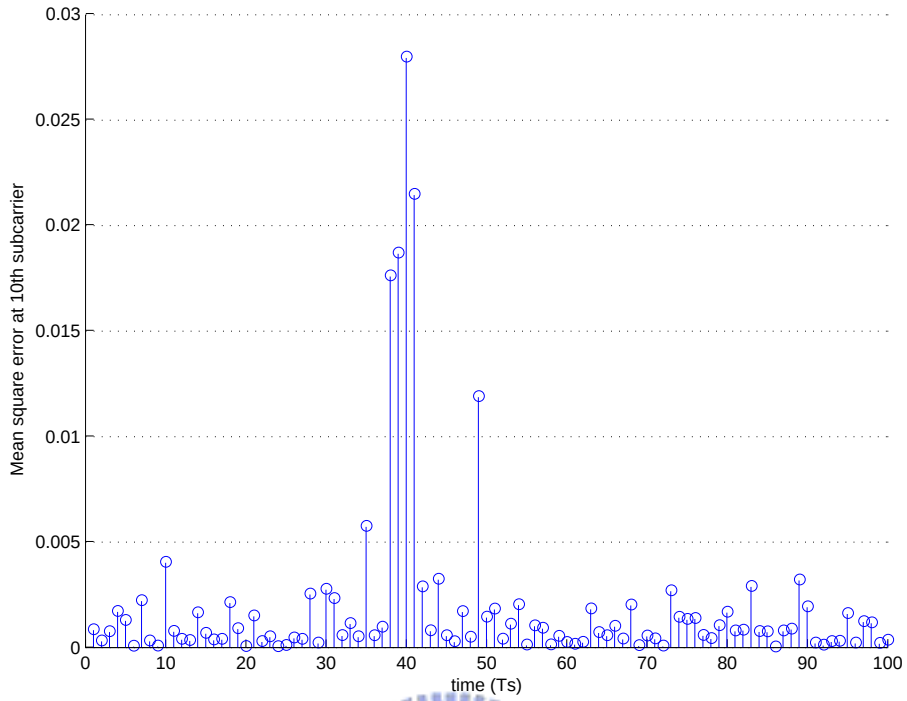

Figure 3.14: Time dependency of channel estimation error.

will be leaked to adjacent subcarrier. A quantitative analysis of the ICI component on each subcarrier can be found in [14]. The index of signal-to-interference ratio (SIR) which is used to represents the effect of intercarrier interference is given by

$$\begin{aligned} \text{SIR} &= \frac{E_s \times E\left[\|ICI(k,k)\|^2\right]}{E_s \sum_{\substack{n=0 \\ n\neq k}}^{N_{FFT}-1} E\left[\|ICI(k,n)\|^2\right]} \\ &= \frac{\sum_{p=1-N_{FFT}}^{N_{FFT}-1} (N_{FFT}-|p|) \times J_0(2\pi f_d \times pT)}{\sum_{\substack{n=0 \\ n\neq k}}^{N_{FFT}-1} \sum_{p=1-N_{FFT}}^{N_{FFT}-1} (N_{FFT}-|p|) \times J_0(2\pi f_d \times pT) e^{j(2\pi/N_{FFT})(n-k)\times p}} \end{aligned} \tag{3.20}$$

where E_s is the average transitted symbols power and $E_s \times E\left[\|ICI(k,n)\|^2\right]$ is the power of transmitted data on subcarrier k leaked to subcarrier n, J_0 is the zeroth order Bessel function of the first kind, and f_d is the maximum Doppler frequency shift.

We use the same 16QAM OFDM system and channel environments as before.

Substituting the system parameters into (3.20), we obtain the theoretical curve of the signal-to-interference ratio (SIR) vs. f_dT_s illustrated in Fig. 3.15.

We also simulate the actual ICI effect for 802.16a uplink channel estimation. The results are depicted in Fig. 3.16. In the case of $f_dT_s = 0.01$, the two curves of block fading and non-block fading are almost overlapping. That means the effect of the ICI is not serious in small Doppler spread. That is corresponding to the result in Fig. 3.15. In the case of $f_dT_s = 0.01$, the SIR, which is about 38 dB, is very small compared with noise power.

However, when $f_dT_s = 0.1$, the SIR is about 18 dB in Fig. 3.15. Then we may predict there is an error floor at about SNR = 18 dB. But in fact, in Fig. 3.16 there is only an unobvious flattening. This means the effect of the ICI is not serious. It only causes a little degradation in performance. We try to analyze the cause of the phenomenon and find out that the average spacing of the adjacent subcarriers in a single subchannel is about $32 \times \Delta f$. However, the main leaked power just leak to limited range about a few Δf. Hence, the adjacent carrier is too far to be affected. That is why the effect of ICI is not severe in Fig. 3.16.

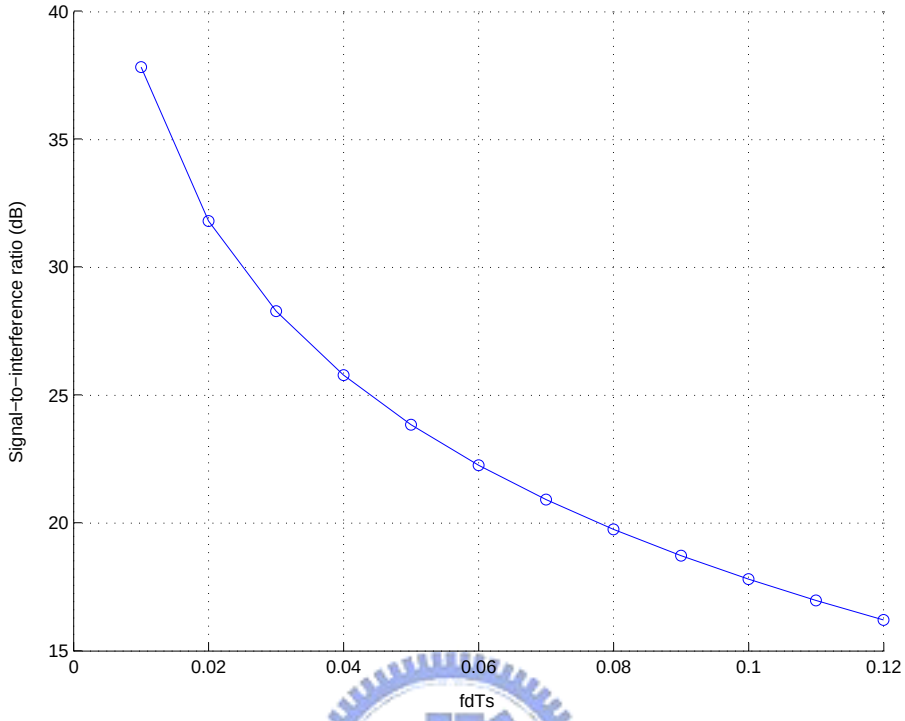

Figure 3.15: Signal-to-interference ratio (SIR) vs. $f_d T_s$.

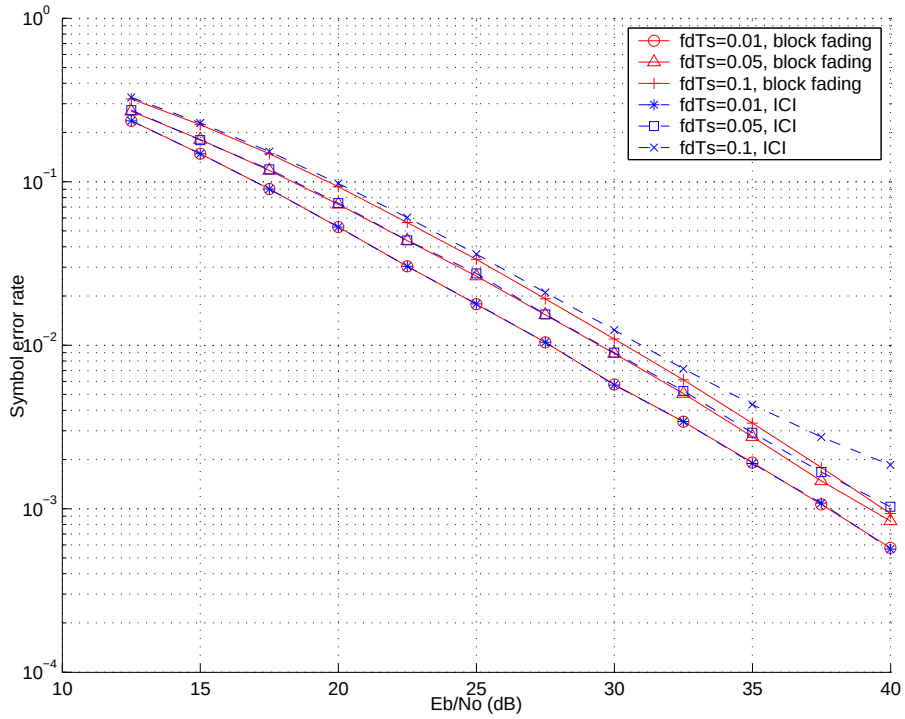

Figure 3.16: Effect of intercarrier interference with different Doppler spreads.

Chapter 4

Tracking of Multipath Time Delays

4.1 Tracking of Multipath Time Delays

The proposed estimator above is based on the assumption that the delay times have been known in advance. In section 3.2, we have mentioned the reason. In order to loosen the restriction, we try to find a way to detect the multipath time delays. However, it is impossible for us to estimate time delays in real time just by using a few pilots. Hence, we modify our goal to track time delays. Suppose we have detected the initial multipath time delays in the beginning of transmission. Therefore we only adjust the time delays of the paths for the following OFDM symbol. Assume that the multipath time delays are slowly time-varying compared with the complex gain of each path. Then we can use the estimate of $\{H_{k_i}(n)\}$ to adjust delay $\{\widehat{\tau}_l(n-1)\}$ to $\{\widehat{\tau}_l(n)\}$.

And in order to avoid the effect of previous time delay, Now we just use those channel gain estimate to adjust the time delay $\widehat{\tau}_l(n)$.

The actual channel gain $H_{k_i}(n)$ on pilot carrier k_i at time n have ever been shown in (3.3) as

$$H_{k_i}(n) \quad = \quad \sum_{l=0}^{L-1} h_l(n) \cdot e^{-j\frac{2\pi k_i \tau_l(n)}{T_b}}, \qquad \text{for } i = 0, 1, \cdots, M-1.$$

Then we get the decision-directed estimate $\widehat{H}_{df,k_i}(n)$ as

$$\widehat{H}_{df,k_i}(n) = H_{k_i}(n) + N_{k_i}(n)$$

where N_{k_i} is channel gain estimation error. We refer to the concept of interpath interference cancellation proposed by [9]. Just taking a designated path into account and cancelling the effects of the other paths from the estimate $\widehat{H}_{df,k_i}$, we get

$$\widehat{H}_{k_i}^{(l)}(n) = \widehat{H}_{df,k_i}(n) - \sum_{\substack{m=0 \\ m\neq l}}^{L-1} \widehat{h}_m(n) \cdot e^{-j\frac{2\pi k_i \widehat{\tau}_m(n-1)}{T_b}}$$

where $\widehat{H}_{k_i}^{(l)}$ is the frequency response of the lth path, and $\widehat{\tau}_m(n-1)$ is the estimated multipath time delay for the m path. Consequently, $\widehat{H}_{k_i}^{(l)}(n)$ can be expressed as

$$\widehat{H}_{k_i}^{(l)}(n) = h_l(n) \cdot e^{-j\frac{2\pi k_i \tau_l(n)}{T_b}} + \widetilde{N}_{k_i}(n)$$

where $\widetilde{N}_{k_i}(n)$ is the sum of the unremovable interference from other paths and channel estimation error $N_{k_i}(n)$. If the magnitude of $h_l(n)$ is much larger than that of $\widetilde{N}_{k_i}(n)$, then the phase of $\widehat{H}_{k_i}^{(l)}(n)$ is similar to that of $H_{k_i}^{(l)}(n)$ where

$$H_{k_i}^{(l)}(n) = h_l(n) \cdot e^{-j\frac{2\pi k_i \tau_l(n)}{T_b}}.$$

Therefore, the time delay of the lth path can be extracted from the phase of $\widehat{H}_{k_i}^{(l)}(n)$ as

$$\begin{aligned} \theta_{k_i}(n) &= \arg\left(\widehat{H}_{k_i}^{(l)}(n)\right) \\ &= \arg\left(h_l(n)\right) - \frac{2\pi k_i \tau_l(n)}{T_b} + \phi_{k_i}(n) \end{aligned}$$

where $\phi_{k_i}(n)$ is phase noise at subcarrier k_i caused by the unremovable interference from other paths and channel estimation error $N_{k_i}(n)$. Accordingly, the estimate of time delay $\tau_l(n)$ can be obtained though $\theta_{k_i}(n)$. There exists a straight line approximation of the phases $\theta_{k_i}(n)$ and it is reasonably accurate:

$$y = -\frac{2\pi}{T_b} a x + b.$$

For the sake of phase noise, the line may not go through all the estimated points $(k_i,\ \theta_{k_i}(n))$. According to [12], the chi-square merit function can be used to measure how well the linear model agrees with the observations as

$$\chi^2(a,b) = \sum_{i=0}^{M-1} \left(\frac{\theta_{k_i}(n) + \frac{2\pi k_i}{T_b} a - b}{\sigma_i} \right)^2$$

where σ_i is the uncertainty of each observation $\theta_{k_i}(n)$ associated with the interference term $\widetilde{N}_{k_i}(n)$. And the merit $\chi^2(a,b)$ is minimized to determine a and b. Because the merit is a quadratic equation, it has a convex surface. Hence global minimum point can be found by taking partial derivatives of $\chi^2(a,b)$ with respect to a and b as

$$\begin{aligned} \frac{\partial \chi^2(a,b)}{\partial a} &= \frac{4\pi}{T_b} \sum_{i=0}^{M-1} k_i \left(\frac{\theta_{k_i}(n) + \frac{2\pi k_i}{T_b} a - b}{\sigma_i^2} \right) = 0, \\ \frac{\partial \chi^2(a,b)}{\partial b} &= -2 \sum_{i=0}^{M-1} \left(\frac{\theta_{k_i}(n) + \frac{2\pi k_i}{T_b} a - b}{\sigma_i^2} \right) = 0. \end{aligned}$$

In fact, the uncertainty σ_i of $\theta_{k_i}(n)$ is hard to analyze. For simplicity, we assume σ_i is equal to 1 for all i. For convenience, define

$$\begin{aligned} \gamma_k &\equiv \sum_{i=0}^{M-1} k_i, & \gamma_\theta &\equiv \sum_{i=0}^{M-1} \theta_{k_i}, \\ \gamma_{kk} &\equiv \sum_{i=0}^{M-1} k_i^2, & \gamma_{k\theta} &\equiv \sum_{i=0}^{M-1} k_i \theta_{k_i}. \end{aligned}$$

Then we can get

$$\begin{aligned} \gamma_{k\theta} &= -\frac{2\pi}{T_b} \gamma_{kk} a + \gamma_k b, \\ \gamma_\theta &= -\frac{2\pi}{T_b} \gamma_k a + M b. \end{aligned}$$

Solving the system of equations, we get

$$\begin{aligned} a &= \frac{\gamma_k \gamma_\theta - M \gamma_{k\theta}}{\frac{2\pi}{T_b} \Delta}, \\ b &= \frac{\gamma_{kk} \gamma_\theta - \gamma_k \gamma_{k\theta}}{\Delta}, \end{aligned}$$

where

$$\Delta = M\gamma_{kk} - \gamma_k^2.$$

According to [12], the formulas above are susceptible to roundoff error. Hence, an alternative is as follows.

Define

$$\begin{aligned} \lambda_i &= \left(k_i - \frac{\gamma_k}{M}\right), \\ \gamma_{\lambda\lambda} &= \sum_{i=0}^{M-1} \lambda_i. \end{aligned}$$

Then, by direct substitution,

$$\begin{aligned} a &= -\frac{1}{\frac{2\pi}{T_b}\gamma_{\lambda\lambda}} \sum_{i=1}^{M-1} \lambda_i \theta_{k_i}, \\ b &= \frac{\gamma_\theta + \frac{2\pi}{T_b}\gamma_k a}{M}. \end{aligned}$$

In fact, the parameter a is the estimate of time delay $\tau_l(n)$ as

$$\widehat{\tau}_l(n) = -\frac{1}{\frac{2\pi}{T_b}\gamma_{\lambda\lambda}} \sum_{i=1}^{M-1} \lambda_i \theta_{k_i}. \tag{4.1}$$

The estimate $\widehat{\psi}_l(n)$ of the phase of $h_l(n)$ is also obtained. as the parameter b:

$$\widehat{\psi}_l(n) = b = \frac{\gamma_\theta + \frac{2\pi}{T_b}\gamma_k a}{M}. \tag{4.2}$$

The concept of time delay tracking is very simple. It can be interpreted as the first order tracking method, because $\tau_l(n-1)$ is used in this algorithm. However, there still exists a problem in implementation. Actually, $\arg\left(\widehat{H}_{k_i}^{(l)}(n)\right)$ is not unique. The probable solutions $\theta_{k_i}(n)$ are

$$\theta_{k_i}(n,m) = \widetilde{\theta}_{k_i}(n) + 2\pi m$$

where $\widetilde{\theta}_{k_i}(n)$ is the principal value of $\arg\left(\widehat{H}_{k_i}^{(l)}(n)\right)$, $-\pi < \widetilde{\theta}_{k_i}(n) \leq \pi$, and m is any integer. Then picking which one is a problem. Fortunately, we can refer

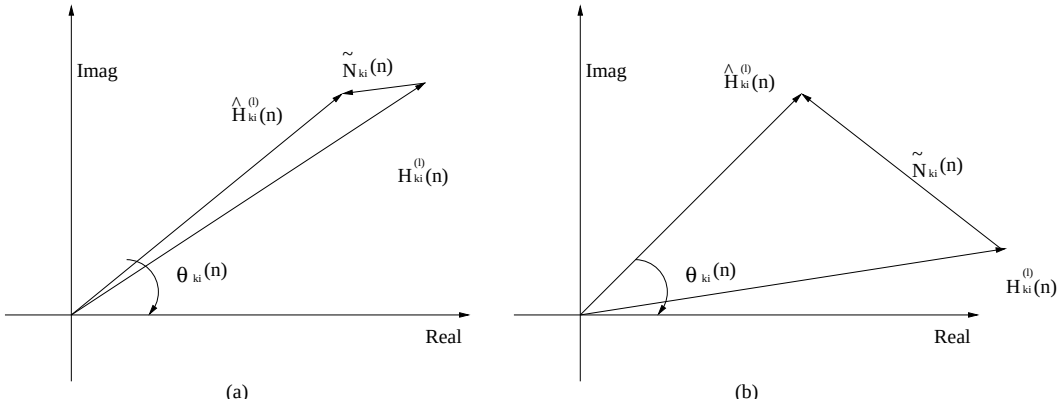

Figure 4.1: Phasor diagrams for the estimate of θ_{k_i} (a) Small interference noise (b) Large interference noise.

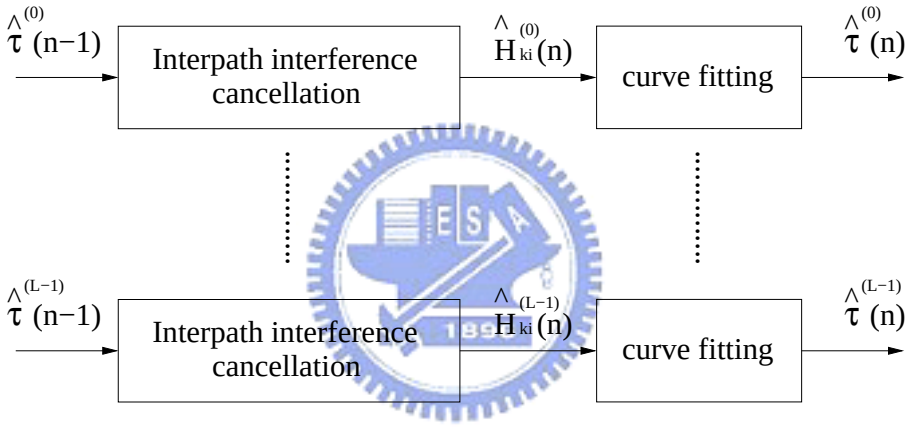

Figure 4.2: Block diagram of multipath time delay tracking.

to the previous value $\widehat{\tau}_l(n-1)$, because we have assumed the delay time varies slowly. Then we can predict that the probable value of $\theta_{k_i}(n)$ is that closest to $\left(\frac{2\pi\tau_l(n-1)}{T_b} + \arg(\widehat{h}_l(n))\right)$. Note that the method have a restriction. That is the power of the lth path must be larger than the power of the unremovable interference from other paths and the channel estimation error, or the phase of $\widehat{H}_{k_i}^{(l)}(n)$ is distorted too seriously to be identified. A block diagram illustrates the operation of delay time tracking shown in Fig. 4.2. In this thesis, we adopt the first order time delay tracking method. Maybe we will take the second order tracking method into account in the future.

4.2 Simulations for Multipath Time Delays Tracking

We assume the initial acquisition of multipath time delays have been done. The simulation only shows the performance of the proposed tracking method. We refer to a channel model in 3GPP, where the lth path delay follows the following time-variation [15]:

$$\tau_l = \varsigma_l + \kappa_l \cos(\lambda_l t)$$

where ς_l is the center location of the lth path, κ_l is the maximum distance away from the center, and λ_l is the coefficient at time t relative to the rate of path delay variation. In general, the multipath time delays are slowly time varying compared with the complex gain of the path in mobile communications. Hence λ_l is chosen as a small value.

In order to investigate into the reliability of the multipath time delay tracking algorithm, the simulations are operated under two different environments. The channel characteristics are shown in Tables 4.1 and 4.2, respectively. The only difference between the two channels is the multipath intensity profiles. In Table 4.1, the multipath intensity profile is assumed to decay linearly. On the other hand, the multipath intensity profile in Table 4.1 has exponential decay. The result of the simulation for channel A is presented in Fig. 4.3, while that for channel B in Fig. 4.4.

We can find that the algorithm operates well at those paths with higher power levels. That is because the power of the noise and the other unremovable paths cover those paths with low power level. In channel A, the power distribution is more uniform than that in channel B. Hence, the algorithm operates well for channel A. For the case of channel B, the power is mainly concentrated in the few initial paths. Then the time delays of the initial paths are well located, but the others are not.

Table 4.1: Characteristics of Simulation Channel A

Tap	ς (μs)	κ	λ	Fractional Power
1	0	0.5	0.01	0.4
2	0.2	0.5	0.01	0.25
3	0.5	1	0.01	0.15
4	1.6	1	0.02	0.12
5	2.3	1	0.02	0.08

Table 4.2: Characteristics of Simulation Channel B

Tap	ς (μs)	κ	λ	Fractional Power
1	0	0.5	0.01	0.5
2	0.2	0.5	0.01	0.32
3	0.5	1	0.01	0.16
4	1.6	1	0.02	0.012
5	2.3	1	0.02	0.008

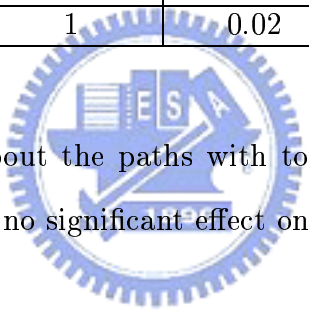

However we may not care about the paths with too low power levels. It can be viewed as noise term and has no significant effect on the channel estimation.

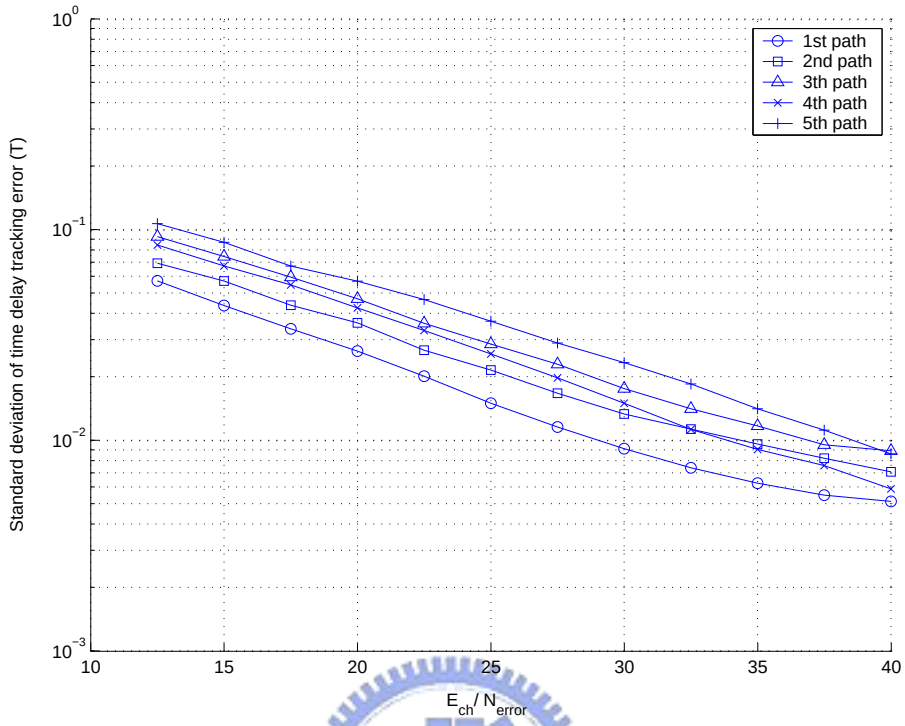

Figure 4.3: Standard deviation of time delay tracking error for channel A.

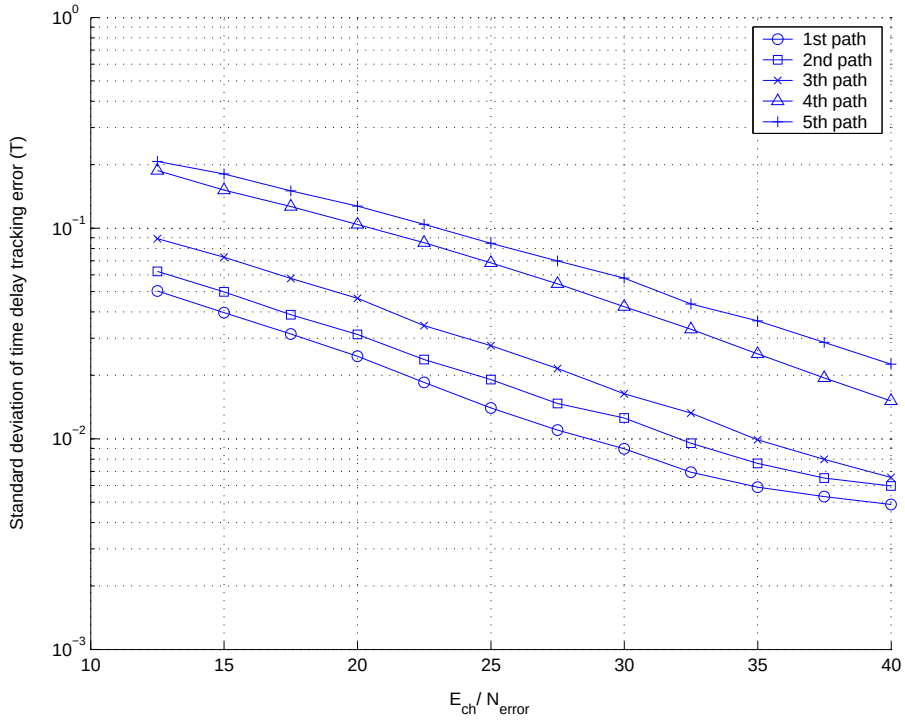

Figure 4.4: Standard deviation of time delay tracking error for channel B.

Chapter 5

Conclusion

We wanted to find a suitable channel estimation method for the IEEE 802.16a. There exists a main problem of too few pilots in uplink channel estimation. That is the major reason which makes the transform-domain estimator useless [8]. Even though the transform-domain estimator has the information of multipath time delays, it also does not operate well due to the noise effect.

In this thesis, a suitable channel estimator for the IEEE 802.16a was proposed. It adopted a multistage architecture in order to reduce the noise power step by step. The main concept was to use the time correlation between adjacent OFDM symbols to suppress the noise effect. Firstly, the least square estimator roughly estimated the channel. Then by using the linear combination between decision-directed and least squares estimators, the noise power was effectively reduced in low SNR. Moreover, we used an adaptive filter to trace the time-variant channel along the time axis so that we got better performance in high SNR. The decision-directed estimator was used as the final stage. It could further reduce the noise power and got more accurate channel estimate. Finally the proposed estimator could achieve significant performance improvement over the least squares estimator about 7–8 dB in a multipath time-variant environment.

According to our simulations, the proposed estimator worked well whether mul-

tipath time delays were at sample spaced positions or not. It was also robust under various multipath intensity profiles. For only one user, the ICI effect was not serious and just caused a little performance degradation in high SNR.

Besides, in order to overcome the channel with time-variant path delays, we modified the multipath time delay tracking algorithm which first proposed by [9]. It was suitable for the channel which had roughly uniform multipath intensity profiles. Sometimes, it failed to track those paths with lower power levels. However, we conjectured that the paths with lower power levels had no significant effect in channel estimation result.

Although, we have presented how to track the multipath time delays, the initial acquisition still remains unsolved. Previously, we assume that the MAC supports to do initial multipath time delays acquisition at the beginning of communication. But actually, the IEEE 802.16a does not deal with initial acquistion. Therefore in the future work, we need to solve the problem of initial multipath time delays acquisition. In addition, the performance of time delay tracking is not good enough. In this thesis, we adopt the first order time delay tracking method. Maybe we will take the second order tracking method into account in the future.

Bibliography

[1] Y.-P. Ho, "Study on OFDM signal description and channel coding in the IEEE 802.16a TDD OFDMA wireless communication standard," M.S. thesis, Department of Electronics Engineering, National Chiao Tung University, Hsinchu, Taiwan, R.O.C., June 2003.

[2] J. A. C. Bingham, "Multicarrier modulation for data transmission: an idea whose time has come ," *IEEE Commun. Mag.*, vol. 28, pp. 5–14, May 1990.

[3] S. B. Weinstein and P. M. Ebert, "Data transmission by frequency-division multiplexing using the discrete Fourier transform," *IEEE Trans. Commun.*, vol. 19, pp. 628–634, Oct. 1971.

[4] D. W. Lin, *Mobile Communication*. Course notes, Department of Electronics Engineering, National Chiao Tung University, Hsinchu, Taiwan, R.O.C., Spring 2003.

[5] J.-J. van de Beek, O. Edfors, M. Sandell, S. K. Wilson, and P. O. Borjesson, "On channel estimation in OFDM system," *IEEE Vehicular Technology Conference*, vol. 2, pp. 815–819, July 1995.

[6] O. Edfors, M. Sandell, J.-J. van de Beek, S.K. Wilson, and P.O. Borjesson, "OFDM channel estimation by singular value decomposition," *IEEE Trans. Commun.*, vol. 46, pp. 931–936, July 1998.

[7] IEEE Std 802.16a-2003, *IEEE Standard for Local and Metropolitan Area Networks — Part 16: Air Interface for Fixed Broadband Wireless Access Systems — Amendment 2: Medium Access Control Modifications and Additional Physical Layer Specifications for 2–11 GHz*. New York: IEEE, April 2003.

[8] Y. Zhao and A. Huang, "A novel channel estimation method for OFDM mobile communication systems based on pilot signals and transform-domain processing," *IEEE Vehicular Technology Conference*, vol. 3, pp. 2089–2093, May 1997.

[9] B. Yang, K. B. Letaief, R. S. Cheng, and Z. Cao, "Channel estimation for OFDM transmission in multipath fading channels based on parametric channel modeling," *IEEE Trans. Commun.*, vol. 49, pp. 467–479, Mar. 2001.

[10] M. Rim, "Optimally combining decision-directed and pilot-symbol-aided channel estimators," *Electron. Lett.*, vol. 39, pp. 558–560, Mar. 2003.

[11] B. Farhang-Boroujeny, *Adaptive Filters: Theory and Applications*. Wiley, 1998, pp. 139–199.

[12] W. H. Press, S. A. Teukolsky, W. T. Vetterling, and B. P. Flannery, *Numerical Recipes in C: The Art of Scientific Computing, 2nd ed.* New York: Cambridge University Press, 1992, pp. 661–666.

[13] Y. R. Zheng, and C. S. Xiao, "Simulation models with correct statistical properties for Rayleigh fading channels," *IEEE Trans. Commun.*, vol. 51, pp. 920–928, June 2003.

[14] J. Li, and M. Kavehrad, "Effects of time selective multipath fading on OFDM systems for broadband mobile applications," *IEEE Commun. Lett.*, vol. 3, pp. 332–334, Dec. 1999.

[15] http://www.rohde-schwarz.com/WWW/Publicat.nsf/article/n169_smiq/$file/n169_smiq.pdf.